Review Article

Suman Kumari Mishra*

Toughening of nanocomposite hard coatings

https://doi.org/10.1515/rams-2020-0049
Received Dec 10, 2019; accepted May 05, 2020

Abstract: For engineering applications, hardness must be complimented with high toughness for applications where high contact loads are there. A good combination of hardness, toughness and low coefficient of friction can be achieved, by suitable tailoring of microstructures of coating in hard nanocomposite coatings. Tribologocal applications require hard coatings with tailored functionalities for different applications; hard nanocomposite coatings are potential materials for such applications. Ti and amorphous carbon based systems have shown more promising material. The present review discusses the nanocomposite hard coatings, mechanism of enhancement of toughness, multilayer hard nanocomposite coatings. Here, mainly Ti and Si based nanocomposite has been discussed as carbon based reviews are available in plenty in literature and well documented. Ti-B-N, Ti-Si-B-C, Ti-Si-B-C-N, Si-C-N, Ti-Al-N, Ti-Al-Si-N, Al-Si-N, Ti-Cr-Al-N, Zr-Si-N and some other similar system nanocomposite hard coatings are important where the gradual and intelligent additions of different elements in hard single component phase provides the combination of hardness, toughness and low coefficient of friction. Some of these systems are discussed. In the end, the future directions of research, Technology,, which are required to achieve tough nanocomposite hard coatings for actual applications are also highlighted.

Keywords: nanocomposite coatings; toughness

1 Nanocomposite hard coatings

Nanoscale dispersion of phases, particles or controlled nanostructure in the composite can introduce new physical properties and can change significantly the properties of the original matrix, which may not be possible in single conventional microstructure or material [1–4]. It can result into very effective change in thermal, optical, electrical and mechanical behavior [5]. In literature, nanocrystalline materials are composed of grains, crystallites, layers of the order of less than 100 nm at least in one direction, but it is not only a theoretical number but should lead to physical importance. The nanocomposite coatings have either two nanocrystalline phases or a combination a nanocrystalline and an amorphous phase. The application of thin films and coatings are the alternative methods to get the required surface characteristics. Corrosion resistance, wear resistance, higher hardness, lower friction, controlled optical properties, aesthetics coatings, and different functional coatings are important. Among them hard coatings are very important. Newer hard coatings are being researched by different methods of deposition techniques to obtain [6, 7] simple monolayer, multilayer or gradient coatings. The limitation is the selection of the coating material. It is impossible to get numerous properties from an ideal coating simultaneously. The application of the nanostructure coatings is a potential solution to meet the complex demand.

Hard nanocomposite coatings with tailored functionality such as low coefficient of friction, wear and oxidation resistance, aesthetic, biocompatibility has many tribological applications [5, 8]. Nanocomposite coatings are isotropic hence, can be applied to three dimensional objects having similar properties [9]. The high density of boundaries between nanometer size grains embedded in the polycrystalline or amorphous matrix results in an increased mechanical resistance.

In nanocomposite hard coatings mechanical and tribological properties may not follow volume mixture rules rather they depend on the synergy of the constituents and grain boundary effect [10]. Along with the hardness, toughness also needs to be good for actual applications. Hardness enhancement apart from toughness has been the primary goal of material scientist all over the world working in the area of nanocomposite hard coatings. Hardness is the resistance to plastic deformation, which predominantly caused by dislocation movement under applied load in a crystalline material. Hard materials usually classified as hardness around 20 GPA. Superhard materials have hardness in the range of 40 GPa, whereas materials having around or more than 60 GPa are called ultrahard materials. Diamond is the hardest material (70-100 GPa)

***Corresponding Author: Suman Kumari Mishra:** CSIR-National Metallurgical Laboratory, Jamshedpur, India-831007;
Email: suman@nmlindia.org; skm_smp@yahoo.co.in;
Fax:91-6572345213

depending upon crystallographic orientation and purity. Cubic boron nitride c-BN on the other hand has hardness of 50GPa, which are conventionally used for different cutting tool and other applications.

Though single layered coatings of transition metal carbides, nitrides and oxides have achieved hardness yet toughness is quite poor to meet the complex demands. Since, single phase coatings fail at high temperature due to decrease in strength, oxidation and decompositions of the phases. Hard coatings with good stability and oxidation resistance are required. Achieving hardness, low friction coefficient, toughness, thermal stability in a coating is very challenging [11].

Nanocomposites have high surface to volume ratio of the reinforcing phase. Super hard nanocomposite coatings have nano-sized sized grains embedded in an amorphous matrix, which influence the hardness of the material. Physical and Chemical vapor deposition processes have been mostly used to deposit nanocomposite coatings. Hardness in the range of 40-80 GPa [12–15], corrosion resistance [16, 17], excellent high temperature oxidization resistance [18–21] and high abrasion and erosion resistance [22–24] have been reported.

The refining of grain size is one of the mechanisms of enhancement of hardness. According to Hall-Petch relation, with the decrease in grain size, the dislocations mobility and multiplicity are hindered leading to increase in hardness. The maximum hardness is achieved at a critical size of the grain below that it softens due to grain boundary sliding and inverse Hall-Petch relation become dominant [19, 25, 26].

The hardness can be improved in two ways:

- Multilayer coatings
- Single layer Nanocomposites

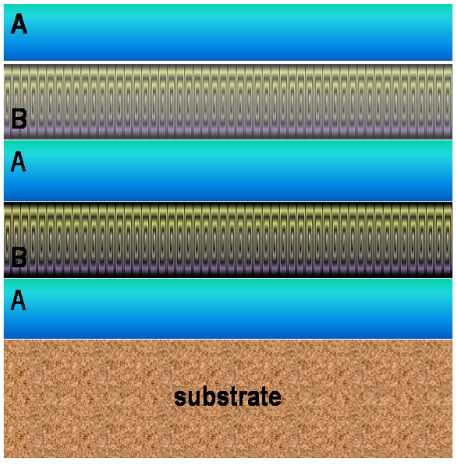

Figure 1: Schematic diagram of Multilayers

Multilayers (shown in Figure 1) with reduced layer (of few nm) thickness and alternate layers of low and high elastic modulus (say B and A respectively) results in high strength films as the dislocations forms in the lower modulus and is hindered at the interface due to repulsive force by high modulus layer when stresses are applied. If one of the layers is amorphous then also the stresses are accommodated. However, to apply multilayers to three-dimensional components and maintaining the right period of layers is very difficult and hence leads to failures.

2 Hardening mechanism in coatings

Nanocomposite hard coating's hardening mechanisms work by providing obstacles for the dislocation movements. Dislocation movement can be hindered by:

- Solid solution hardening
- Grain boundary hardening
- Compressive stress hardening
- Age hardening

The high strength achieved is also due to high cohesive energy and high elastic modulus. The multiplication, movement and pile up of dislocation in crystalline materials and growth of micro cracks affect the strength of material. The dislocations move across the barrier and newer dislocation forms, once the applied stress is more than critical value, and continues until accumulated stress field is balanced by the applied stress. The decrease in crystallite size also results in increase in hardness, which is given by the Hall-Petch relationship between the strength in terms of the critical stress σ and grain size d

$$\sigma_c = \sigma_0 + kd^{-1/2} \tag{1}$$

Where, σ_c = critical stress, σ_o = bulk stress, k = material constant

The immiscibility of the two phase's nanograins and amorphous matrix in the nanocomposite induces hardness in the coating. The amount of matrix, size and shape, dispersion of the nanocrystalline phase influence the hardness. A thermodynamic segregation, similar to spinodal decomposition is required for achieving enhanced hardness.

The nanocrystalline amorphous composites show improvement in strength due to reduced dislocations in very small crystallites and reduction of stress due to presence of amorphous phase. The dislocation in the crystalline phase cannot propagate in the amiorphous phase due

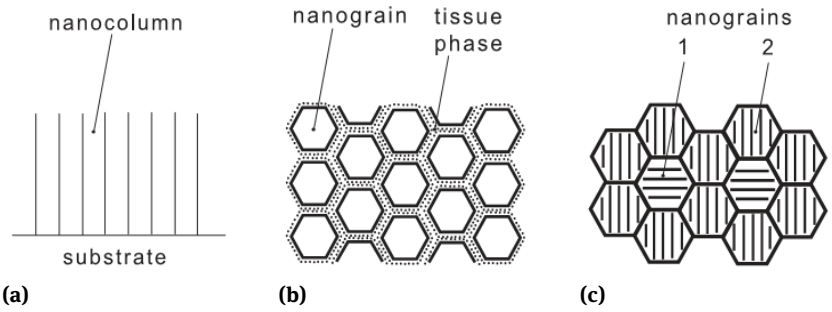

Figure 2: Schematic diagram for nanocomposite coatings with enhanced hardness (a) Columnar structure (b) Nanograins surrounded by tissue phase (c) mixture of Nanograins with different orientation [27]

to lattice misfit and vice versa. The cohesive energy is also high in high strength amorphous and nanocrystalline phases. In small crystallites the energy and multiplication of dislocation is very high and they are repelled towards grain boundary leading to further inhibition of dislocation movement [27]. The dislocation movement restrictions in the amorphous matrix show no or very less plastic deformation and have brittle behavior.

The nanocomposite films for high hardness can have the:

a) Columnar nanostructure composed of grains assembled in nanocolumns with sufficient amount of second phase, Figure 2(a).
b) Dense globular nanostructure having nanograins surrounded by amorphous phase, Figure 2(b).
c) Nanostructure with mixture of different oriented grains of different materials., Figure 2(c) [2]

3 Toughening of nanocomposite hard coatings

For engineering applications, hardness must be complimented with high toughness. High fracture toughness is necessary for applications where high contact load applications are there. The component or the substrate materials deforms significantly. A tough material is of high strength with good elastic recovery. A high elastic modulus and high yield strength gives higher hardness, but the introduction of ductility in hard materials is very challenging. Toughness is also the resistance of formation of crack and its propagation and is the ability of the material to absorb energy during deformation up to fracture. High resistance to crack formation, crack deflection and high energy absorption under applied stress is essential for a tough coating, which helps in preventing chipping, flaking or catastrophic failure.

In order to obtain high hardness in nanocomposite coatings, the microstructures are designed such that plastic deformation is prohibited by preventing dislocation movement and grain boundary sliding. For glasses and ceramics, when the applied stress exceeds the critical value for a particular crack size, micro cracks starts growing and leads to brittle failure of the materials as per Griffith's theory. However, in nanocrystalline composites the crack growth is hindered and very small in the range of to 2-4 nm. Hence, nanocomposite coatings also provide toughness and low friction along with hardness.

Hard nanocomposite coatings with enhanced toughness should be very elastic, exhibit a low plastic deformation, resilient with an enhanced resistance to cracking.

Hard, tough and resilient coatings follow Hooke's law $\sigma = E.\ \epsilon$;

Here, σ is the stress (load); ϵ is the strain (deformation).

For higher elastic deformation the Young's modulus E must be reduced. The coatings should have lowest value of the Young's modulus E (σ = const) at a given hardness H. However, it is very difficult to meet.

Hard and tough materials exhibit both elastic and plastic deformation. A tough material shows the stability to cracking at higher strain *i.e.* $\epsilon 1 \ll \epsilon \ll \epsilon$ (max) and higher hardness can be obtained if ϵ (max) is achieved at higher σ. whereas; fully resilient hard coatings show lesser hardness with no plastic deformation and have high elastic recovery. This leads to more resistance to the cracking. Figure 3 shows the schematic of different properties in the stress and strain curve, showing the different behavior [28].

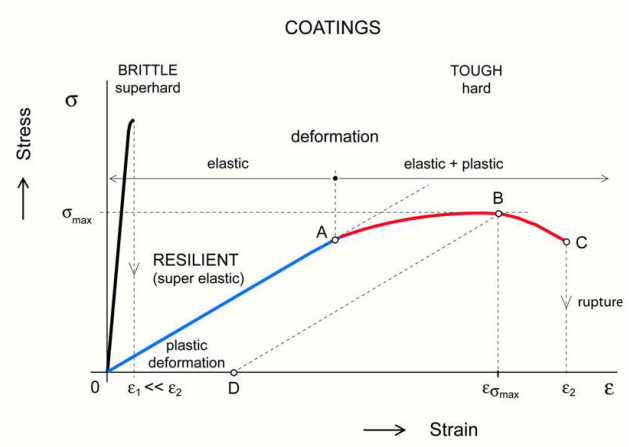

Figure 3: Stress vs strain curves of superhard (brittle), hard (tough) and hard (resilient) coatings [27]

4 Designing hard and tough nanocomposite coatings

The grain boundary hardening is one of the mechanisms for enhancing the hardness and is applicable for coating also. When the grains are of the order of 10 nm or so the enhancement of hardness are observed even more as the multiplication and mobility of the dislocations are hindered (Figure 4) [19].

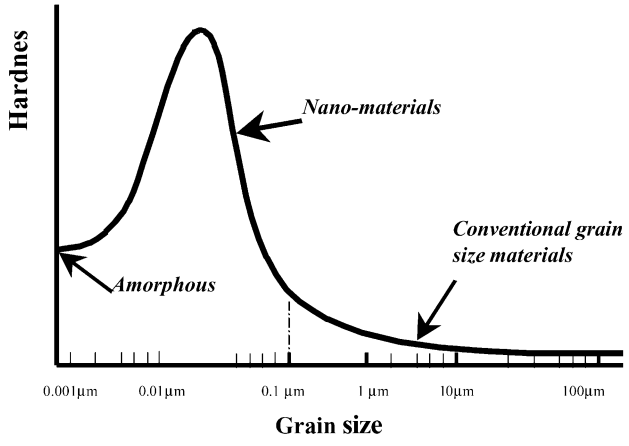

Figure 4: Hardness of material as function of grain size [29]

The complex boundaries accommodate coherent strains and prevent cracking & defect formation. Hence, multiphase structures can be designed suitably to have more interfaces with high cohesive strength. High fracture toughness in the nanocomposite coatings can be obtained with nano-size grain structure, deflection of cracks by secondary phase, and pinning of cracks at boundaries. The grain boundary properties such as structure and angle are important for movement of dislocations that determine the mechanical properties of the nanocomposites. A small amount of diffusion and grain boundary sliding are required to improve toughness of the nanocomposite coatings. A variety of hard materials can be used in nanocomposite coating design [27, 29].

Ternary, quaternary or more complex systems with amorphous phase of higher strength as matrix and nanocrystalline phase increase the grain boundary strength. The bonding in the composite also decides the hardness and toughness. Figure 5 shows the bond triangle showing change in properties with the change of chemical bonding.

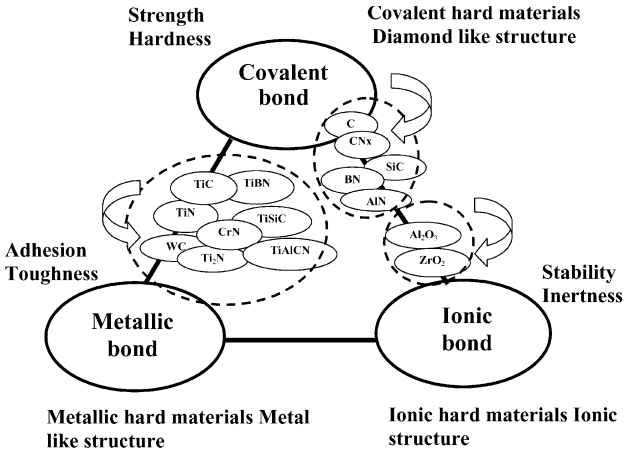

Figure 5: Hard materials in the bond triangle that affect the properties due to change in chemical bonding in nanocomposite coating [30]

5 Material selection for hard coatings

For selection hard coatings following issues are very important:

- The coating and substrate interface as it affects the adherence and interaction of the substrate with the layer.
- Composition and microstructure that determines the properties such as hardness, strength, internal stress, fracture tougghness and thermal stability.
- Layer surface interaction conditions for actual application.

The material selection are tough as obtaining high hardness with good adhesion with minimum substrate-layer interface interaction, high toughness simultaneously is difficult [30–32].

Nanoscale multilayer increases the hardness and toughness. Alternating layers of high and low elastic modulus can achieve high shear strength coatings as it inhibits dislocation formation and mobility [33–35]. The periodicity of multilayer could be related to hardness as 1 / (periodicity)$^{-1/2}$ like Hall-Petch relation in Al/Cu and Al/Ag multilayers [36]. Few other researchers also have shown that some metal-ceramic and ceramic-ceramic laminates followed the similar Hall-Petch relationship [30, 37–44]. The layers must have sharp interface with 5-10 nm periodicity for such coatings [45–47]. However, it is difficult to apply uniform periodicity on three dimensions with uniform thickness. Hence, nanocomposite single layer that has the similar advantages along with other additional improvement in properties. Such coatings are not critically dependent on thickness or substrate geometry.

The superhard nanocomposite coatings generally have 3-10 nm grains embedded in an amorphous matrix separated by 1-3 nm [14, 28, 48–54]. The nanocrystalline phases are nitrides, carbides, borides, and oxides, while the amorphous phase may be metal or ceramics such as silicon nitride and diamond-like carbon (DLC). The nanocrystalline phase should have strong interaction with the matrix phase to impart super-hardness. Some of the systems which have shown high hardness's are TiN/a-Si_3N_4 [48, 55, 56], W_2N/a-Si_3N_4, VN/a-Si_3N_4, TiN/c-BN [49, 57], TiN/a-(TiB_2+TiB+B_2O_3), TiN/TiB_2 [58], TiC/TiB_2 [59], TiN/Ni [60], ZrN/Cu [61], ZrN/Y [62], TiAlN/AlN [63], CrN/Ni [52], Mo_2C/a-(carbon+Mo_2N) [64], TiC/DLC [65, 66], and WC/DLC [67, 68]. Among the carbon matrix systems, The DLC with no hydrogen showed the higher hardness 30-40 GPa [39, 40, 65–68].

The hardness enhancement is due to the suppression of dislocation movement in small grains and the narrow amorphous space between grains make strains incoherent [39, 40, 51]. In the absence of dislocation activity, Griffith's equation for crack opening can be written as,

$$\sigma = \left(\frac{4E\gamma_s}{\pi a}\right)^{1/2} \tag{2}$$

Where, E, γ_s and 'a' are the elastic modulus, surface energy of the interface of grain and matrix and initial crack size, which is considered as equal to average grain size, respectively [57]. The increase in the elastic modulus, surface energy of the combined phases, and decrease in grain size can enhance the strength. The elastic modulus is inversely dependent on grain size as in nanometer grains lattice incoherence strains and the high volume of grain boundaries are present. The Griffith-Orovan model [69] may describe the composite strength of metal / ceramic nanocomposites as:

$$\sigma = \left(\frac{4E\,(\gamma_s + \gamma_p)}{\pi a}\,\frac{r_{tip}}{3d_a}\right)^{1/2} \tag{3}$$

Where, γ_p, r_{tip}, da are the work of plastic deformation, curvature of the crack tip, interatomic distance respectively. The crack tip blunting improves the material strength and the lower elastic modulus of metals reduces strength as compared to ceramics.

Composite designs with increased elastic modulus and hardness do not necessarily achieve high toughness. When the stresses exceed the strength limit, dislocation movement hindrance and the crack opening takes place. The moving crack energy is balanced by friction loss and breaking of bonds. The stored potential energy is released by crack opening and the kinetic energy is gained leading to the crack propagation [30, 70]. A stored stress results into potential energy release through the moving crack and crack can propagate through macrocracks causing brittle fracture. However, in nanocomposite coatings the higher grain boundary volume limits the initial crack sizes and helps to deflect, split, and terminate growing cracks. In superhard coatings, the dislocation activity is restricted but that is one of the mechanisms to get tougher material. In addition to ductility, a tough coating must have high elastic modulus and high hardness so that strain relaxation and crack termination occurs. Combination of these properties in a coating results in high cohesive toughness. It is also important to prevent failure at the coating -substrate interface by increasing interface toughness and adhesion.

6 Tough multilayer coatings

Toughening can be achieved in many ways in multilayers [9, 14, 45, 46, 71]. The crack splitting, deflection at the grain boundary and interface of multilayers, stress concentration reduction and energy dissipation at the interface by plastic deformation and stress relaxation are the different mechanisms which acts in multilayers. While interfaces in ceramic / ceramic multilayer can deflect cracks and relax stress, they can also initiate brittle fracture. This is critical when the adjacent layers have very different elastic modulus and chemistry, which causes a sharp change in the stress field across the interface. In the absence of good chemical bonding and adhesion, coating failure is initiated. Depending on the applied stress field and individ-

ual layer properties (*e.g.*, elastic modulus, yield strength, residual/induced stress, and thickness), the coating may fail by interfacial crack propagation due to shear, tensile, compressive stresses [72, 73].

To improve fracture toughness and reduce the brittle failure a graded interfaces between the coating and substrate and between layers are required. The WC-TiC-TiN graded coating [74] showed considerably less wear than single layer hard coatings. Hydrogen free DLC coating on steel has a very high hardness and large residual compressive stress, however, the adhesion problem remains. The graded compositions in Ti-TiN-TiCN-TiC-DLC for hydrogenated DLC [75, 76] and Ti-TiC-DLC for hydrogen-free DLC [77] showed the enhanced adhesion with good toughness. The graded coatings showed five times higher strength in scratch and no brittle failure was observed [78]. The tribological properties can be further enhanced by using graded approach with multilayer and nanocomposite architectures. The DLC coating with Ti under layer showed much higher toughness than single layer DLC coatings though reduction in hardness was also observed [78]. The low elastic modulus ductile layer in coating system, allow dissipation of crack energy at the crack tip by plastic deformation, is an efficient way to improve toughness. However, in mulitilayers the process controls to ensure the correct compositions, structures, and properties during growth is tough due to difficulties in managing multilayers [79].

7 Tough nanocomposite coatings

An alternative to multilayers coatings, a single layer having fine grains of a hard, high yield strength phase into a softer matrix also gives toughness as ductility is introduced [50, 80–82]. In single layer nanocomposite coating, the high volume of grain boundaries with a crystalline or amorphous transition across soft matrix interfaces reduces dislocation activity and limits the crack size. It also deflects and terminates growing cracks [22, 83]. In single-phase nanocrystalline systems, grain boundary diffusion [84] and grain boundary sliding [84–88] provide the plasticity. Multiphase or multicomponent structures [89–93] also improve the toughness by grain boundary sliding. The grain boundary sliding happens due to the presence of amorphous phase at boundaries, high angle grain boundaries and low surface energy [84, 85, 94].

The graded interface layer between the substrate and crystalline / amorphous composite coating additionally enhances the adhesion strength of the nanocomposite coatings to relieve stresses [95–97]. The 3-10 nm hard crystalline grains in amorphous matrix due to large volume fraction of grain boundaries provides toughness through grain boundary sliding by reducing the dislocation mobility and arresting and diverting the cracks [35, 98–101]. The primary differences between superhard and tough coating designs are selection of a matrix phase with a lower elastic modulus and larger range of grain size of nanocrystalline phase in tough coatings. The design of amorphous-nanocrystalline with higher cohesive interface (adhesive) and functionally graded interface for higher toughness in a single coating is shown in Figure 6 [102].

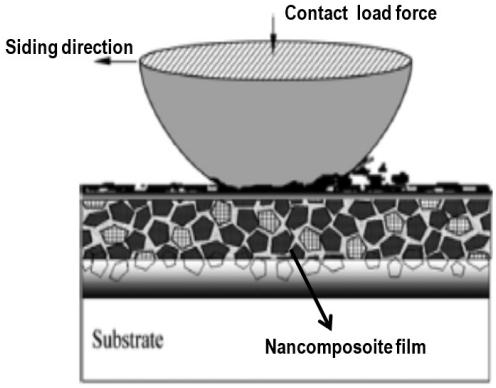

Figure 6: Schematic of a tough nanocomposite coating for cohesive and adhesive toughness [19, 102]

Nanocomposite coatings can be designed suitably to achieve high hardness, toughness, and low friction into a single coating. The inclusion of a solid lubricant film amorphous or poorly crystalline in nanocomposite coatings minimizes friction forces and surface reactions with the environment. A lubricious transfer film on surface is formed at the tribological contact, which can self-adjust with each environmental change [98, 103, 104]. Figure 7 presents a

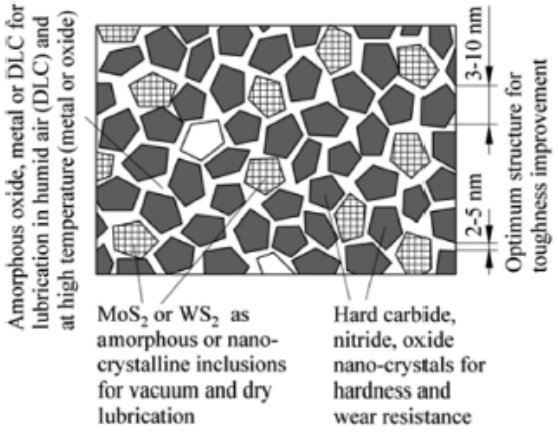

Figure 7: Conceptual design schematic of self surface adaptive nanocomposite tribological coating [19, 102]

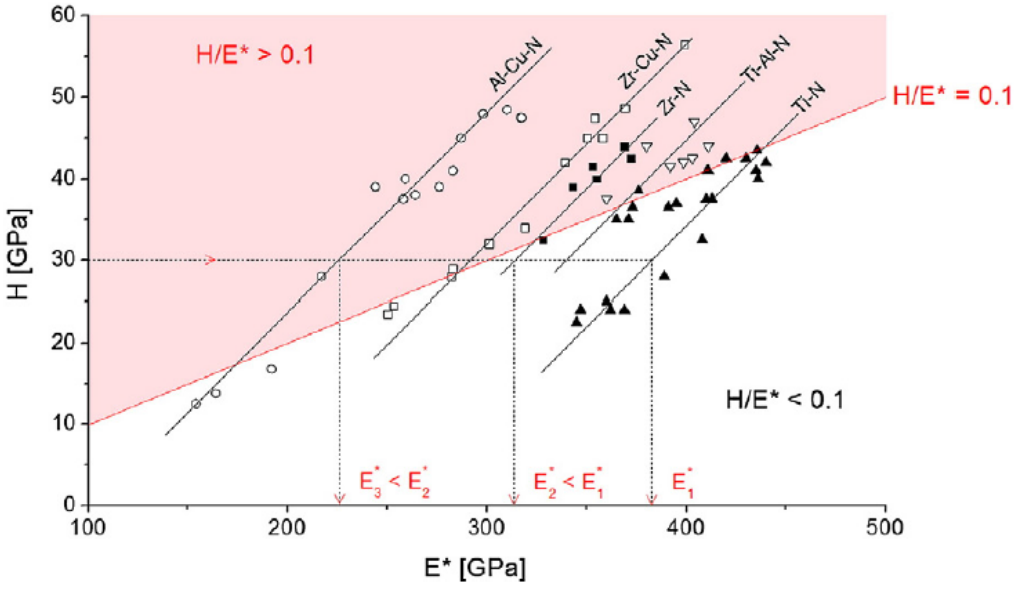

Figure 8: Control of E* and H of different binary nitrides [27]

schematic of a nanocomposite coating design that can exhibit the hardness, toughness and low coefficient of friction with self-adaptive during contact wear [19, 102].

The hard nanocomposite coatings with high toughness should satisfy high H/E ≥ 0.1 and a high value of the elastic recovery. This can be achieved by addition of suitable elements in the base material. The H/E dependence of different systems with different elemental addition is shown in Figure 8 [27]. The straight line H/E*= 0.1, divides the H–E* plane in two regions one H/E*>0.1 and other H/E* <0.1. The effective Young's modulus E* coating can be different for the similar hardness H depending on the composition and phases formed. Hard coatings satisfying the ratio H/E*≥ 0.1 show higher toughness, as it enhances the resistance to plastic deformation and distribute the load more effectively. However, it is a difficult task as hardness H and the effective Young's modulus E* are directly proportional generally.

The possibility of mixing hard and lubricious phases in thin nanocomposite coatings has been explored. Reports on producing TiN/MoS_2 composites by chemical vapor deposition [105, 106], TiB_2/MoS_2, TiB_2/C, TiC/DLC, WC/DLC and TiN/MoS_2 composites by magnetron sputtering [107–109], hybrid deposition of WC/DLC/WS_2 and YSZ/Au/DLC/MoS_2 composites by laser ablation and sputtering have shown good combination of toughness and low friction coefficient. They were also found stable at high temperatures in the range of 300°C-500°C and different environment [110–117].

The nanocrystalline and amorphous soft phases of MoS_2, DLC, WS_2, embedded in the nanocomposite coatings act as seal from the environment. During sliding processes, the stress and frictional heat cause changes in chemistry and structure. A graphitic-like transfer layer is formed in DLC reducing the friction coefficient to 0.10 to 0.15 and wear loss is decreased in humid atmosphere. However, in humid environment MoS_2 or WS_2 transfer layers is not favorable as they have high friction coefficient, but are very good for dry air, nitrogen and vacuum environments. Different carbides, nitrides, borides, and oxides in combination with carbon can be used as nanocomposite coatings for lubrication in ambient conditions, whereas MoS_2 and WS_2 for dry and vacuum environments.

The addition of small atoms such as carbon, nitrogen, boron in the hard ceramic coating has shown enhancement of mechanical properties leading to the suitable combination of phases in the nanocomposite coatings. A good combination of hardness, toughness and even low coefficient of friction can be achieved. Significant microstructure and crystalinity of the films change leading to the formation of fine grained nanocomposite films. There are many systems which have been researched. Ti based and amorphous carbon based systems have shown more promising material for applications. Here, mainly Ti and Si based nanocomposite shall be discussed as carbon-based reviews have already been discussed and well reported in literature in detail [65, 118–121]. The nanocomposite coatings of Ti-B-N, Ti-Si-B-C, Ti-Si-B-C-N, Si-C-N, Ti-Al-N, Ti-Al-Si-N, Al-Si-N are important, where the gradual and intelli-

gent additions of different elements in hard single component phase provides the combination of hardness, toughness and low coefficient of friction. These systems shall be discussed further.

8 Toughness and hardness enhancement of Nanocomposite Silicon carbonitride Si-C-N hard coating

8.1 Single layer Si-C-N nanocomposite

The ternary nanocomposite material Si-C-N is high temperature oxidation resistant polymer derived ceramics (PDCs) [122, 123]. It has functional properties of polymers with the mechanical, chemical durability of ceramics. The silicon oxycarbide (SiOC) and silicon carbonitride (Si-C-N) are two families of polymer-derived ceramics. Both of them have very high crystallization temperature of the order of 1500 to 1600°C. The X-ray diffraction patterns are though featureless but are not strictly amorphous. A short-range structural feature is there. The crystallization gets retarded because of extremely low atomic mobility in polymer-derived Si-C-N [124, 125]. Apart from high temperature oxidation resistance, the hardness as well as high temperature stability of Si–C-N phase exceeds individual SiC and Si_3N_4. The electronic band gap of 2.5-3.8 eV makes it potential as a wide band gap and dielectric material. More importantly, the stability of β-C_3N_4 with comparable diamond hardness has been achieved in ternary silicon carbonitride. These properties make silicon carbonitride a promising material for prospective applications such as MEMS, hard protective coatings, and electronic materials [126–131]. The amorphous Si–C–N transforms to thermodynamically stable crystalline phases, by shrinking and cracking and a phase separation into C-rich, SiC-rich, and Si_3N_4 rich amorphous domains takes place [124, 132]. These structures depend on the silicon and nitrogen ratio irrespective of the carbon content in the film.

Si-C-N being a ternary structure, solid solution of the formation of α-and β-C_3N_4, Si_3N_4 and SiC has been found. With the addition of small amount of Si in C-N matrix small crystallites of β-C_3N_4 10 nm sizes have been found to nucleate in the amorphous Si-C-N matrix and show better mechanical properties. However, the addition of excessive amount Si led to the formation of amorphous phase [122, 123, 129–131, 133]. The electrical conductivity (DC) for Si-C-N at room temperature is $10^4\,\Omega^{-1}\mathrm{cm}^{-1}$, due to formation of sp^2 carbon atoms. The refractive index of oxidized Si-C-N is 1.4 and that of nonoxidized is 2.07. The band gap is adjustable between 2.86 to 5.0eV. The extinction coefficient is 10.0 for oxidized and 2.0 for nonoxidised samples. Fracture toughness of 2.1 MPa$\sqrt{m}$ and 3.3-4.3 MPa$\sqrt{m}$ have been reported by indentation crack length and single edged notch beam method respectively. These materials compared to monolithic ceramics see better creep behavior. The Si-C-N has shown stability up to 1600°C and it remains in the amorphous state up to 1500°C [122, 123, 125, 128–136] due to low oxygen diffusion, cross-linking of Si, C and N atoms, and covalent bonding. Additionally, the smaller grain size, larger interface fraction & amorphous layer between grain, compressive residual stress, and solid solution of different phases show enhanced mechanical behavior in Si-C-N nanocomposite coatings. The formation of SiC, Si_3N_4 and C_3N_4 phases gives the higher hardness of Si-C-N coating.

The Si-C-N coating both crystalline and amorphous have been deposited on various substrates by different methods [137–165]. The different processes are plasma and ion assisted deposition [137–139], Pulsed high energy plasma deposition [140], Chemical Vapor Deposition [137], sputtering [158, 164, 165], microwave and electron cyclotron resonance PECVD [161, 163], ion implantation [165], pulsed laser deposition [157], HWCVD [144], electrochemical methods [143], remote plasma CVD [149] and rapid thermal Chemical vapor deposition. Nanocrystalline Si_2CN_4 has been prepared by metal organic CVD. The incorporation of 10% Si_3N_4 in graphite through PLD the CSi_xN_y films show hardness around 23 GPa, but elastic modulus decreased from 464 to 229 GPa. Amorphous Si-C-N films synthesized by CVD showed the hardness in the range of 22–38 GPa with 224–289 GPa stiffness [161, 163]. Sputtered Si-C-N films are mainly amorphous consisting of Si–N, C–N single, C=N double, and C≡N triple bonds.

The Si-C-N films formed along the SiC–Si_3N_4 tie line exhibit the highest load carrying capacity in lubricated sliding [166]. In dry sliding the premature coating failure occurs due to their brittleness coupled with a high coefficient of friction. The carbon rich Si-C-N films showed good wear resistance and low coefficient of friction due to formation of graphitic structure. However, their ability to withstand high pressures is reduced [163]. The gradient films from silicon rich to carbon rich at the surface showed good wear properties in dry reciprocating sliding and high load carrying capacity [166, 167].

SiCN film growth by magnetron sputtering is highly influenced by plasma parameters. Author and group have reported magnetron sputtered Si-C-N film of around 4 μm showed different hardness deposited at different pressure. The hardness was 4445 Hv at 1 Pa, 3918 Hv at 5 Pa and 2545

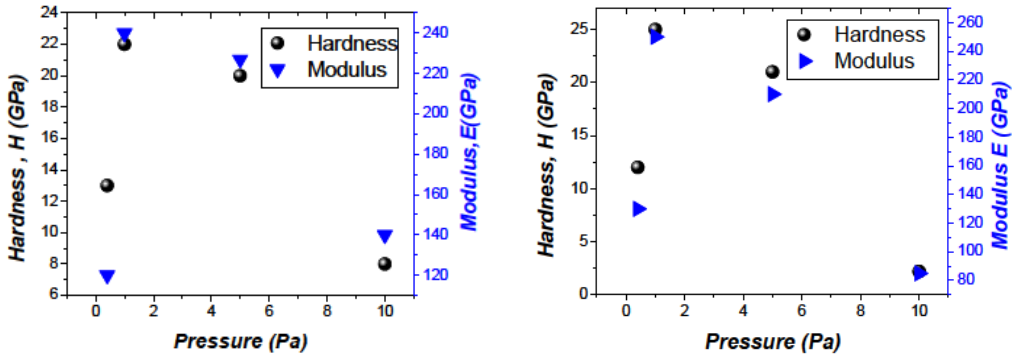

Figure 9: Variation of maximum average nanohardness and elastic modulus with pressure for Si-C-N coatings deposited on (a) Silicon and (b) Steel substrates.

Hv for 10 Pa [168]. The hardness and modulus measured by nanoindentation of these films on silicon and steel substrate also showed effect of deposition pressure similarly (Figure 9).

The reason for obtaining the highest hardness was the formation of hard phases like β-C_3N_4 along with β-Si_3N_4 in the pressure range 1-5 Pa and lowering of particle size to about 2-20 nm. A decrease in the hardness and modulus values on the other hand at higher and lower pressures 4 and 10 Pa respectively were due to formation of graphitic phase [168, 169]. The substrate temperature played a good role for tailoring the modulus and hardness. The hardness increased from 2238 Hv at room temperature to 4445 hV for 500°C substrate temperature. At 600°C, it decreased to 3166 Hv as at higher temperature additional graphitic phase formation took place along with hard β-C_3N_4 and β-Si_3N_4 phases in the amorphous Si-C-N matrix [170]. The deposition source whether DC (Direct current) or RF (Radio frequency) also affects the hardness and toughness of the film. RF source resulted into higher hardness compared to that of DC deposited Si-C-N film. Table 1 shows the nano hardness values for coatings deposited on silicon and steel substrates in both RF and DC mode. The depositions were carried out at around 400 watt in both RF and DC mode at deposition pressure 1 Pa and thickness of Si-C-N film was around 4 µm for both cases. The film in the RF mode deposition had finer grains; absence of elemental Si and the presence of higher amount of Si_3N_4 and C_3N_4 phases were observed as compared to DC deposited films. The slower deposition rates in RF allow sufficient migration of the atoms to form the different phases [170].

The total work done (W_T) is a sum of elastic (W_E) and plastic work (W_P) during indentation and can be estimated from the area under load-depth curve, as shown

Table 1: Hardness and modulus of different mulitilayer stacked SiCN nanocomposite hard-soft coatings

Layers	Hardness (GPa)	Modulus (GPa)	H/E
Hard	32	265	0.12
Soft	9	115	0.078
Hard-soft	25	265	0.094
Soft-hard	36	335	0.11
Hard-soft-hard	36	310	0.11

in eqn. 4

$$W_T = W_E + W_P \tag{4}$$

The DC deposited Si-C-N film showed higher plastic work done than that of the RF deposited one. The elastic recovery was more in case of RF sputtered coatings. Hence, the RF deposited film was tougher than DC deposited Si-C-N coating. The holding depth at 105 mN was also higher in DC films (30nm) compared to RF films (5nm) [Figure 10], proving it to be better creep resistant too. The linear unloading in load -depth curve was observed in the DC films which was absent in the RF film, which is associated with buckling of the coating. Hence, RF deposited Si-C-N films were tougher and mechanically more stable than the DC deposited films.

The applied normal load vs. coefficient of friction (c.o.f) plots is an effective mean to measure the coating adhesion [171, 172] in scratch experiment. The critical load, the load at which the film fails as the indenter slide through, is the point where change in the coefficient of friction [173, 174] happens. The RF deposited Si-C-N films showed much higher critical load 17.5 N as compared to that of DC deposited one which was 2 N.

The scratch tracks showed tensile cracking on both the coatings which is through thickness cracking, but the extent of failure of the DC film was more compared to the RF film, circular flakes (Figure 11c,d) coming out at higher loads is seen in DC mode film, which was absent in RF deposited film. The nanoscratch studies also confirmed higher scratch resistance in RF deposited films and higher elastic recoveries [175, 176].

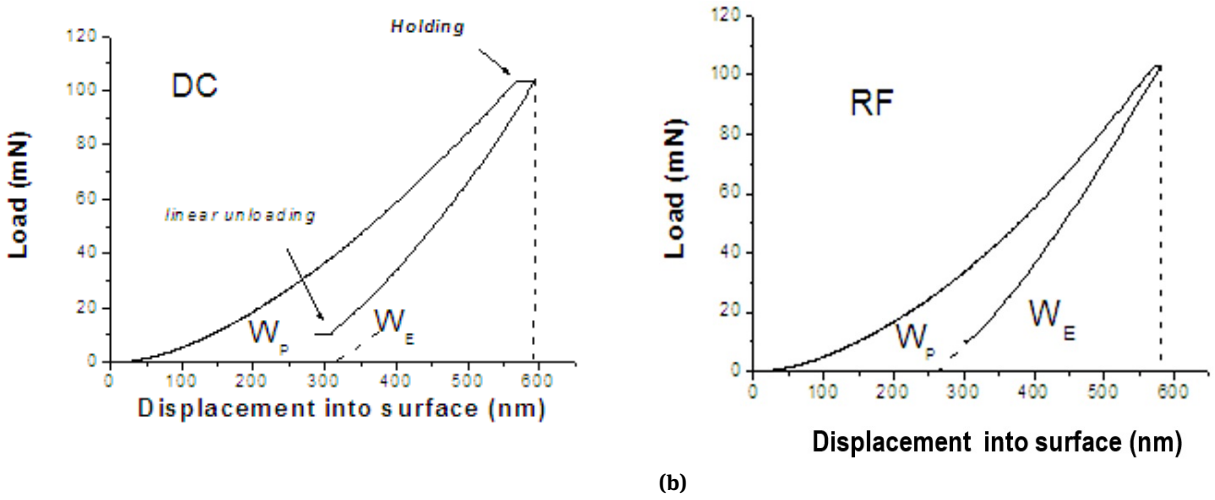

(a) (b)

Figure 10: The nanoindentation load depth curves for (a) DC and (b) RF modes Si-C-N coatings on silicon substrates [170]

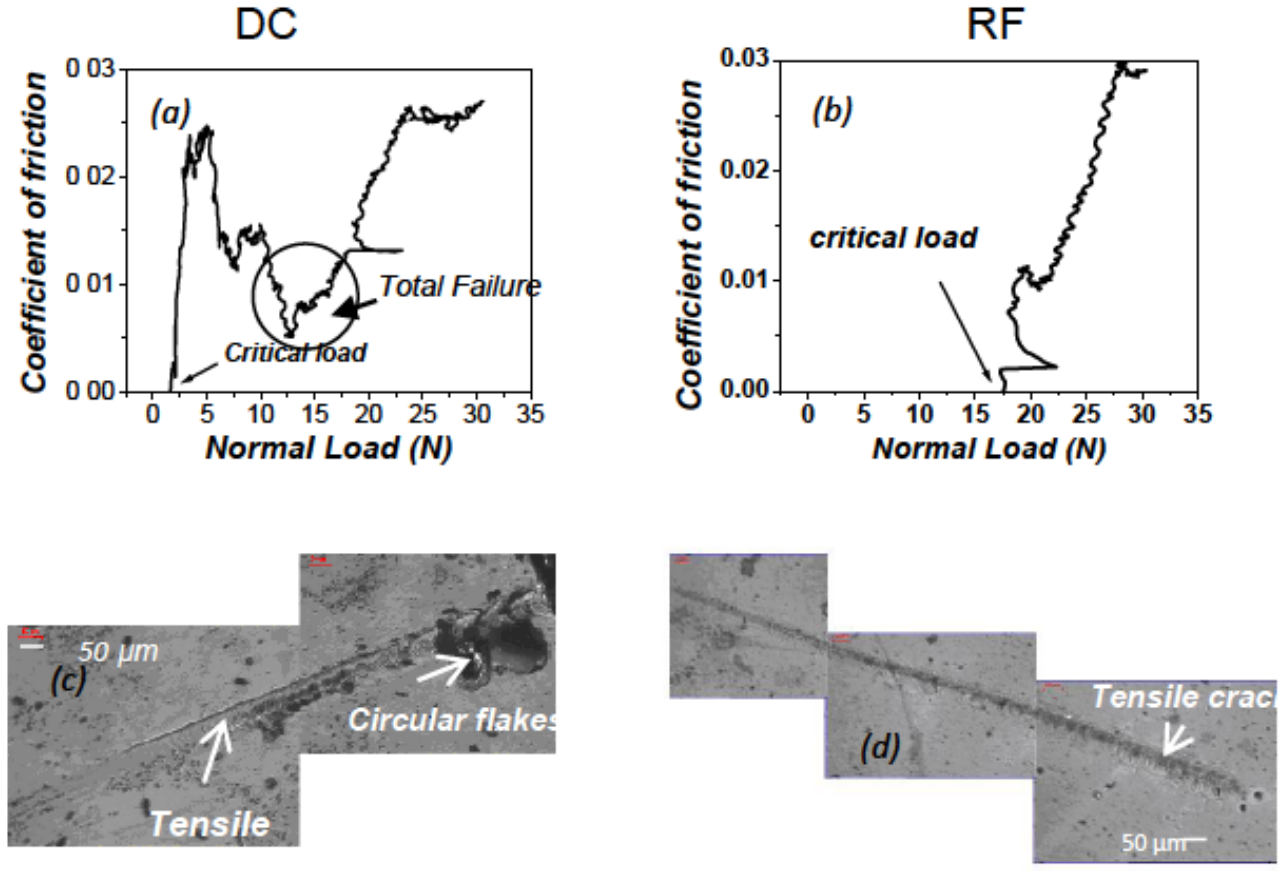

Figure 11: Coefficient of friction vs. Normal load plots for Si-C-Films deposited in (a) DC and (b) RF modes and corresponding scratch tracks [170]

The ultimate toughness is also dependent on the coating-substrate combination. Figure 12, 13, 14 shows the hardness and load-displacement curves with and without Si-C-N coatings on Si and SS substrate. Different power laws express the loading curve during nano indentation, which is the function of the load, indenter geometry, roughness of the indenter and sample. The sharp Berkovich indenter is used for thin coating so that the contact stresses are high enough to cause yield in the coating before the substrate. The initial contact behaves like the spherical tip and is elastic. At very low load it can be expressed as P=kh, h is the displacement. Further, the load varies as displacement raised to the power of 3/2 ($P=kh^{3/2}$), which is typical Hertzian elastic behavior due to the interactions of the roughness of the indenter and the substrate (Figure 12b).

As load increases, the indenter behaves like truncated cone as sloping sides come into contact then plastic deformation is initiated and further behaves like a sharp cone with increase of the load. Here, the load varies parabolically ($P=kh^2$) with displacement and full elastic–plastic deformation takes place below the indenter [177].

At low loads, the elastic response of the hard coating is more which is unlikely to be happening in case of the bare substrates. At higher loads, the substrate effect increases due to the deformation of substrate [177–179].

Si substrate, which is harder than steel, shows elastic recoveries as was observed on Si-C-N coated substrate, except during unloading the substrate showed pressure induced phase transformation signature, a kink in the unloading curve (shown by arrow) [Figure 12, 13b]. An elastic recovery of 50% was observed in both. Whereas, a large

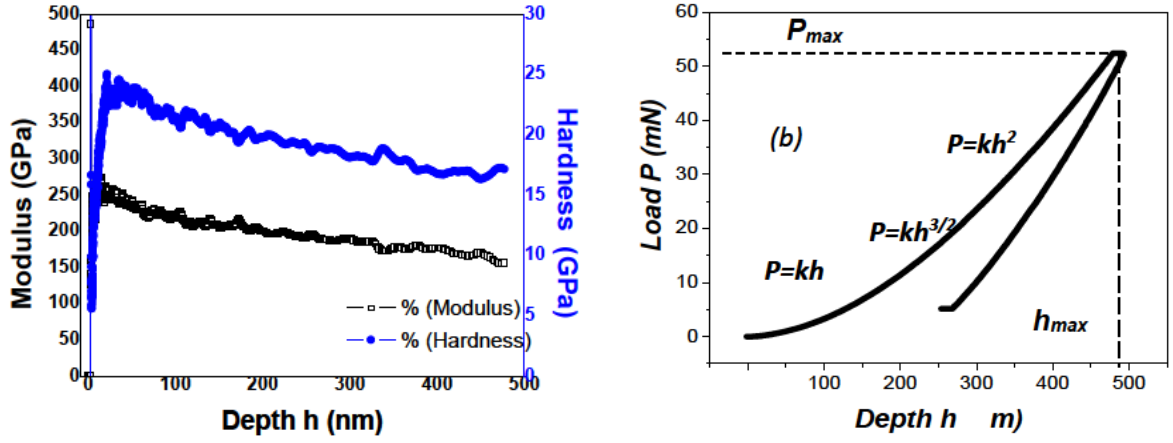

(a) (b)

Figure 12: (a) Hardness and modulus variation with indentation depth and the corresponding (b) Load-depth curve for Si-C-N coatings deposited on Silicon substrates [178]

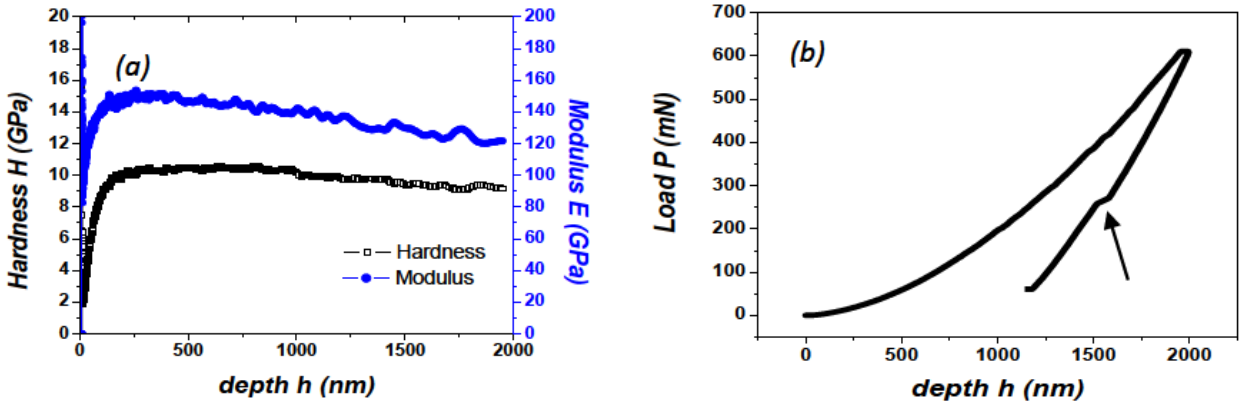

(a) (b)

Figure 13: (a) Hardness and modulus variation with indentation depth and the corresponding (b) Load-depth curve bare Silicon substrates

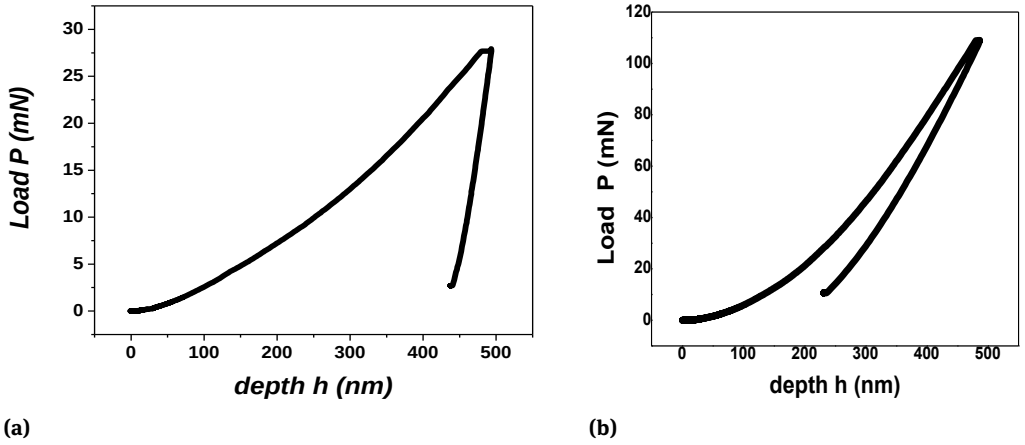

Figure 14: Load-depth curve for bare steel and SiCN Coated steel

plastic deformation takes place when only bare 304 SS substrate is indented (Figure 14a). The elastic recovery was very less (10%) with hardness and modulus 4 GPa and 200 GPa respectively. Si-C-N nanocomposite coated steel increased the elastic recovery to 50% with H and E with 26 GPa and 250 GPa respectively (Figure 14). Hence, SiCN coatings can improve the surface and resistance to failure largely and depend on the nature of substrate and coating combination.

Thus for increasing hardness and toughness deposition parameters such as pressure, power, mode of electrical source RF and DC, substrate and film combination such as soft or hard substrate over which hard film is deposited influences the toughness of SiCN Coating. RF depositions showed a better elastic recovery, scratch resistance and gave a tougher film compared to DC deposition under similar condition. Soft substrates used for hard coating deposition showed plastic deformation primary due to not the film failure rather substrate deformation is induced before film, where as hard substrate showed brittle failure.

8.2 Multilayer nanocomposite SiCN coatings

The alternating layers improve the fracture toughness by crack inhibition at layer interface and by inhibiting the crack propagation by tough material. The deformation accommodation is increased by alternating soft and hard layers. The thin hard layers slide by shear deformation of low modulus layers [180–182]. However, the two dissimilar layers have interface stresses, thermal and lattice mismatch. The deposition pressure and nitrogen to argon ratio play a dominant role in the formation of different phases and results into a hard film (>20 GPa) or soft (<20 GPa) in nanocomposite coatings. The deposition of alternate hard and soft layer of same Si-C-N material by suitable adjustment of C to N ratio circumvents the problems of interface stresses, thermal mismatch, and lattice mismatch. S.K.Mishra *et al.* by depositing Si-C-N hard and soft alternate layers by maintaining different pressure during deposition have addressed this issue [183]. The soft films were deposited at 10 Pa during deposition and hard films were at 1 Pa with 99:1 and 1: 99 nitrogen to argon ratio respectively. The soft films had larger particle size (100-200 nm), whereas the hard films had very fine structures. The hardness of both hard and soft nanocomposite individual layers were 32 and 10 GPA respectively. The modulus was 265 and 115 GPa for hard and soft layers respectively. Both soft and hard layer were deposited for 2 hrs each at 150 watt and their thicknesses were 1.7 and 2 μm respectively. Same 2 hr duration was maintained for developing hard-soft-hard layers deposition for each layer [183].

The cross-sectional studies interface of the trilayer film having sequence hard-soft –hard three layers on silicon is shown in Figure 15. The hard layer was found amorphous and had sharp boundary with soft layer and subsequently with the upper hard layer. No delaminations were found. The middle layer showed nano columnar growth morphology and had larger particle size compared to hard layer. The middle soft layer had more nitrogen compared to hard layer, which is expected as was the tailored condition during deposition.

Nitrogen incorporation in the film reduces the hardness due to formation of soft phases. The slower growth rate due to nitrogen species gives, enough mobility to ad atoms leading to more structured growth. The deposition rate was much higher for hard layers compared to soft layer. The hardness and modulus as measured and H/E

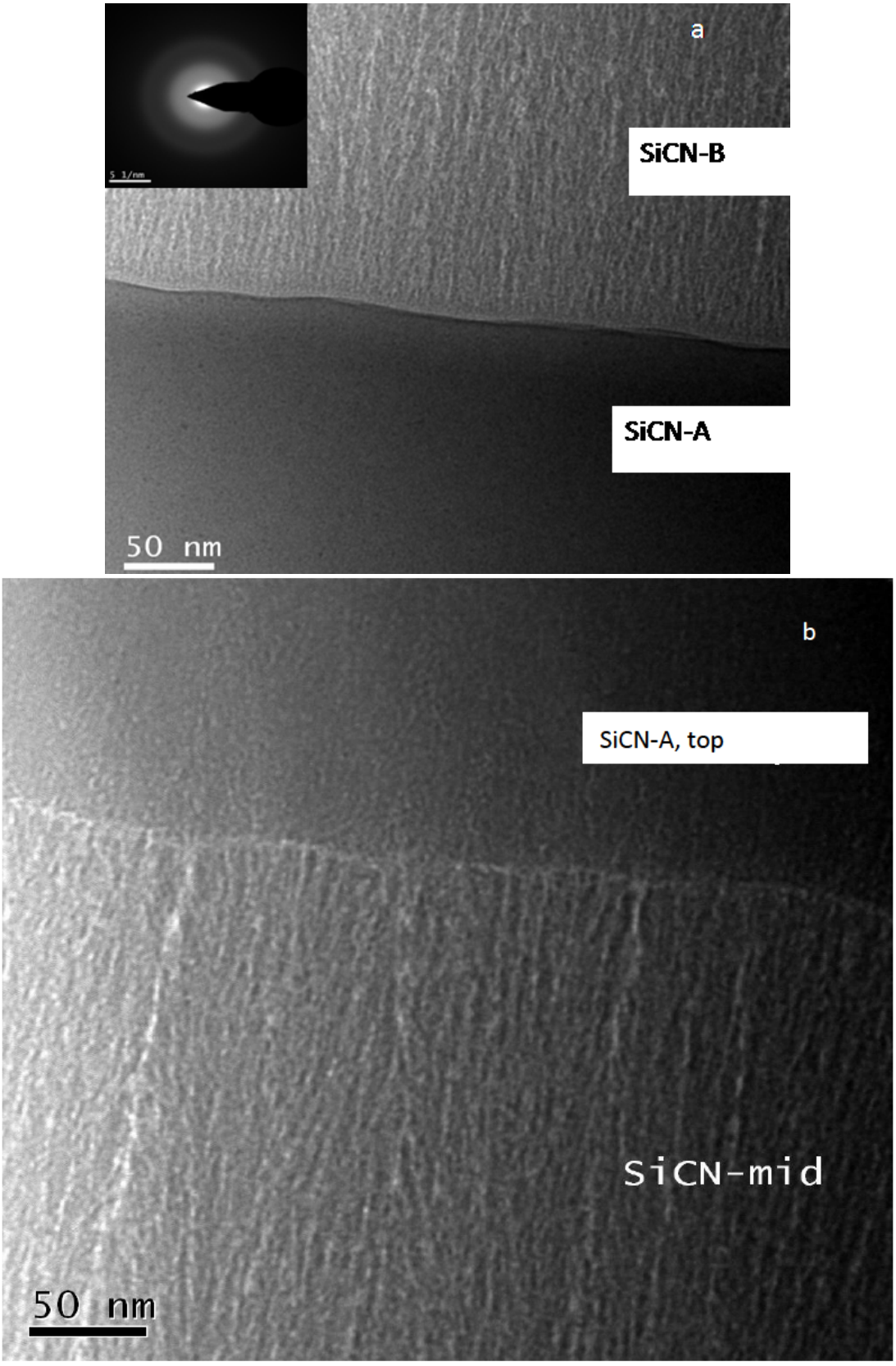

Figure 15: Cross section TEM microstructure and interface of SiCN coating at different interfaces of trilayer hard-soft-hard sequence [183]

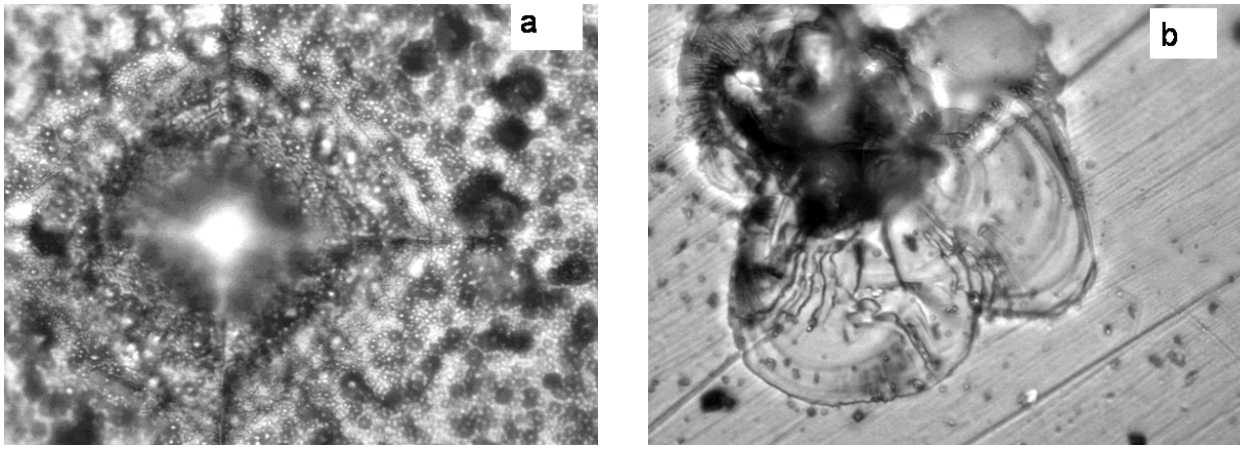

Figure 16: Optical picture of Indent for trilayered SiCN coating (a) and single layer SiCN Coating (b) [183]

are given in Table 1. It was observed that underlayer soft layer gave higher elastic recoveries and higher surface hardness and modulus compared to the individual layered films [183].

The trilayer film had better resistance to loading than single layer hard coatings. A soft layer in between had significant effect on building resistant behavior against indentation on both the substrates silicon and steel. Multilayers deposited on steel did not show failure even at 2000gf, rather pileups were developed due to plastic deformation of the SS (Figure 16), but no spalling or cracking was observed. However, such failure took place for single hard coating on steel, spalling was clearly visible. Hence, a soft layer film increased the load bearing capacity of the film. In multilayer soft -hard structure load distribution happens so that stresses are managed resulting into tougher film. Also, the columnar growth of the soft SiCN layer beneath or in between hard layers increased the toughness due to the stress distribution and deflection.

The Fracture toughness of the trilayer nanocomposite SiCN hard- soft-hard layer was found around of 9.5-10 MPa $m^{1/2}$, which is significantly higher than the reported values for ceramic nanocomposite and single phase films. The fracture toughness of single layer Si-C-N film was around 3.5-4 MPa $m^{1/2}$.

Thus, multilayer hard and soft nano composite of the same system can be made to increase the toughness of the same nano composite coating by suitably adjusting the carbon and nitrogen ration in SiCN film. This is also applicable to other systems where role of C, N, B are very important and they dictate the ultimate properties of the coating, J. Musil *et al.* has also shown such in Zr-Si-O system [184]. Such multilayer will be free from two dissimilar material stresses that are normally developed in multilayer films leading to spallation and other failures due to lattice mismatch, thermal stresses.

9 Toughness and hardness enhancement of TiB_2 coating by adding different elements and forming nanocomposite hard coating

9.1 Nanocomposite Ti-B-N

Titanium diboride (TiB_2) is a high temperature material with high melting point (>3000°C), good electrical conductivity (electrical resistivity 13×10^{-8} Ωm), high thermal conductivity (65-110 W/mK), high hardness (25-35 GPa) and elastic modulus (500 GPa), high temperature oxidation resistance (<1000°C) and harsh environment stability [185]. Hence, TiB_2 is very potential material for tribological coating applications [186], optical mirrors, diffusion barrier in microelectronics [187, 188], high temperature strain gauge [189], surface coatings on first wall components, cathode materials [190–192]. TiB_2 has hexagonal crystal structure [193]. Different techniques have been used for deposition of TiB_2 coatings such as chemical vapor deposition [187, 194–205], pulsed laser deposition [206–208], dynamic ion mixing [209] and magnetron sputtering [210–217]. Though TiB_2 has high hardness, the coatings accommodate high compressive residual stress during deposition limiting its applications. The macro stress in the films can be reduced by controlling the energy imparted to the growing film by ion bombardment. Kunc *et al.* [217] has

reported that the intrinsic macrostress decreases with increasing ratio T_s/T_m (where Ts is the deposition temperature and Tm is the melting point) and for Ts/Tm >0.25, it is lower than approximately 0.3GPa. Substrate dependent stress was observed by Isao *et al.* [218] and they found that the TiB_2 films have a tensile stress depending on the substrate on which the films were deposited. A low tensile stress was observed on graphite substrates whereas it was high on the copper substrates. Sanchez *et al.* [219] have observed that the internal stress of the TiB_2 films is compressive in nature and increases with the increase in the film density.

The deposition parameters, such as, temperature, pressure, substrate distance, rotation, substrate angle, DC or RF sputtering, all play an important role in the structural evolution and TiB_2 film properties. The deposition pressure has significant effect on the properties of sputtered coatings [220]. The TiB_2 film transforms to the disordered crystalline or amorphous structure from crystallized (001) texture of hexagonal system as the deposition pressure is increased during sputtering. Substrate rotation during deposition led to the difference in the orientation of the films [221]. A large variation in the hardness of the TiB_2 films from 20 GPa to 60 GPa is reported for films deposited using different deposition methods such as PECVD, sputtering etc. [214, 217, 222–225]. Nitrogen incorporation made the films better resilient and have been studied as Ti-B-N System [58, 226–229].

The TiB_2, TiN, c-BN hard and h-BN soft phases are found in Ti-B-N coating system [226, 230–232]. This gives immense flexibility to tailor the mechanical properties by controlling the coating deposition conditions. Variety of methods, such as PECVD [192, 228, 233–235], thermal CVD [236, 237], MCVD [238], ion plating [239, 240], arc evaporation [241] and sputtering [242–251] have been used to obtain Ti-B-N coatings with different composition and structures. Among the various methods, most of the researchers have focused on the deposition by PVD methods and mostly by magnetron sputtering.

The Ti-B-N films deposited by reactive magnetron sputtering have shown a transition from the crystalline to completely amorphous microstructure with the increase in the nitrogen flow rate [227, 245, 249]. With the increase in the nitrogen flow the bonding of boron atom changed from titanium to nitrogen, thus favoring the formation of amorphous BN [252]. A dual phase of BN and TiN was observed. The formation of the h-BN was also reported for films deposited in Ar/N_2 gas mixture at high nitrogen partial pressures along with the formation of the TiB_2 and TiN phases [249, 253–257]. The formation of amorphous Ti-B-N films has also been reported [258–260]. In contrast, the Ti-B-N films deposited by non-reactive sputtering of segmented target of TiN-TiB_2 resulted in the formation of nanocrystalline phases of TiB_2 and TiN [248]. A large variation in the hardness 12 GPa to 80 GPa was reported for Ti-B-N films [227, 245–260]. High hardness was reported for films with TiN and TiB_2 or TiB phase formation. The formation of h-BN is favored with increasing nitrogen content and the hardness was found to decrease.

The wear resistance of the Ti-B-N coating with the TiN-TiBx composition was observed to be an order of magnitude higher than TiN [261]. The incorporation of boron into TiN decreased the coefficient of friction and specific wear rate. Also, the wear mode changed from abrasive wear to dominant adhesive one. When B content was increased to 42 at% an inverse trend occurred due to the formation of hexagonal BN phase [262]. The Ti–B–N and TiN/BN/TiB_2 multilayer thin films show very less self-lubrication [263]. The coefficient of friction decreased for lower nitrogen content but gradually increased with higher nitrogen content in the plasma [242].

One of the most important issues of the coating is the reliability. This assumes importance where the coatings are hard and brittle, such as TiB_2. The property governing this issue is fracture toughness. Fracture toughness of the brittle materials can be calculated using the following relationship to within 40% accuracy based on maximum indentation load, $9P_{max}$ and the crack length c [208, 209]:

$$K_c = \beta \cdot \left(\frac{E}{H}\right)^{1/2} \cdot \frac{P_{\max}}{c^{3/2}} \tag{5}$$

Where, β is an empirical constant dependent on indentor geometry. It has value 0.032 and 0.016 for cube corner and Berkovich & Vickers indenter respectively. E and H are the elastic modulus and hardness respectively. A cube corner indenter with a semi-angle of 35.3° introduces cracks at very shallow depth of the film, which is beneficial for measuring the toughness of the film. The Berkovich indenter significantly lowers the cracking thresholds minimizing the substrates influence, due to large angle of tip. The fracture toughness was found to be of the order of 0.598±0.05 $MPa{\cdot}m^{1/2}$. The fracture toughness determination from energy based models from nanoindentation p-h curve is another method which also takes into account the thickness of the film [211], besides the radial crack method. The pop-in from P-h curve, which occurs due to fracture in film, gives the energy released during fracture. An enlarged view of pop-in is shown in the loading curve (Figure 17). If the fracture would not have taken place the loading curve path would have been AD rather than ABCE. The crack formation changes the path of the loading curve. So

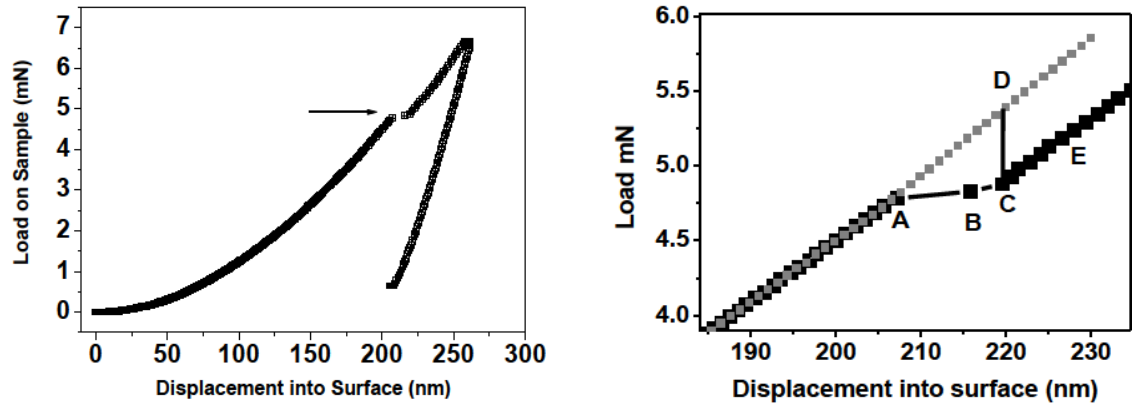

Figure 17: a) P–h plot with cube corner indenter for TiB_2-Si. The fracture event is shown by the arrow b) Enlarged plot of the pop-in where the area ABCD gives the energy released due to the crack formation [264]

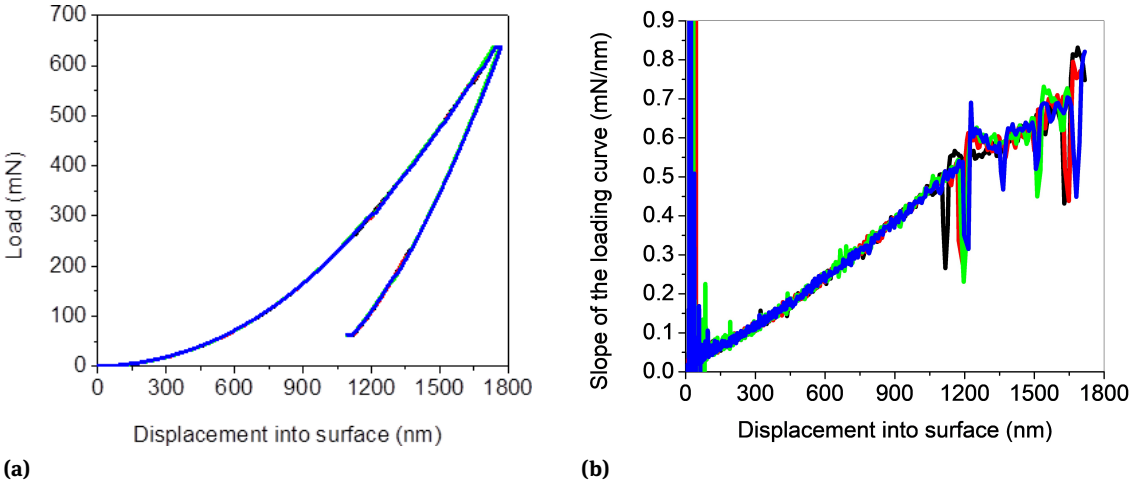

Figure 18: p-h and Slope of the loading curve Vs. displacement for the film 93:7 Ar:N_2

the energy difference before and after crack generation is estimated as area ABCD.

The fracture toughness is calculated using the following equation 6 [27]

$$K_c = \left[\left(\frac{E}{(1-\nu^2)\,2\pi C_R}\right)\left(\frac{U}{t}\right)\right]^{1/2} \qquad (6)$$

Here, E, ν, U, t, C_R are the elastic modulus, Poisson's ratio, strain energy released, thickness of the film and the radius of the circumferential crack respectively. The total length of ring-like crack is used when circumferential crack takes place for the measurement of toughness. Here, the sum of the radial cracks at three corners of the cube corner indenter is considered and the fracture toughness gave similar K_c = 0.578±0.11 MPa·$m^{1/2}$ [264].

The authors have reported Ti-B-N deposition under different N_2: Ar ratios using a single TiB_2 target by DC magnetron sputtering with different Nitrogen content. In order to investigate the effect of nitrogen on toughness, the first derivative (slope) of the nanoindentation curves with depth were analyzed. The Ti-B-N films deposited on silicon substrates undergo deformation upon indentation. The fracture events will be marked by discontinuities. The load at which these discontinuities occur indicates the critical load for fracture of the films. The p-h plots and slope of the loading curve with depth of the Ti-B-N films are shown in Figure 18. The curve is very smooth up to a displacement of 1100 nm. After 1100 nm, marked discontinuities are observed. From the load-depth curve the corresponding load for these discontinuities is found as 250 mN. These discontinuities are a result of the fracture events. Films deposited

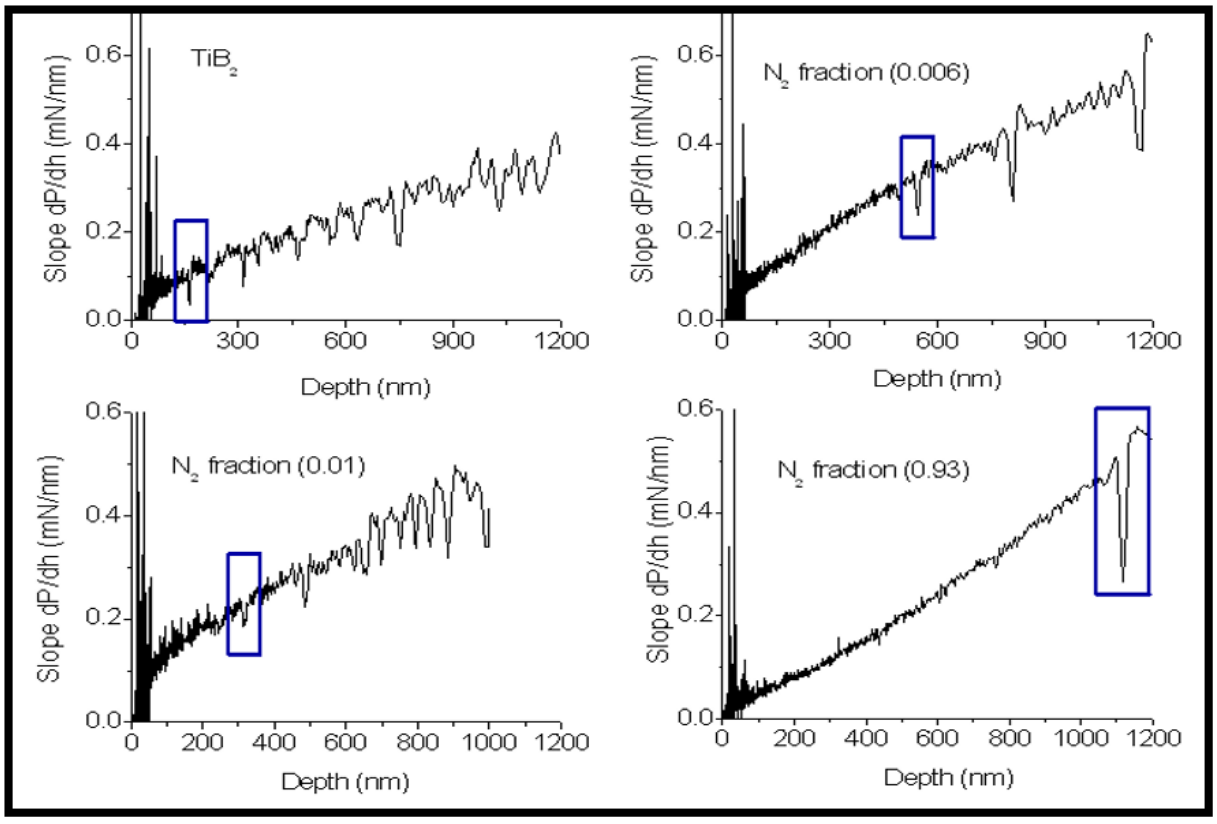

Figure 19: Slope of the loading curve vs. depth for Ti-B-N films at different N fraction in the film [265]

at different Nitrogen content the slope of loading curve versus depth or displacement is shown in Figure 19. The 1st discontinuity varied with nitrogen content, which is the critical load for that film. The critical load varied with nitrogen content, for pure TiB_2 it was 31.4 mN, which was much less than TiBN film. This shows that the by suitable incorporation of nitrogen in TiB_2 the toughness of TiB_2 film can be enhanced, but the hardness decreases (Figure 20).

Fracture toughness using the method of Lawn [193] of TiB_2 film and for the film deposited at N_2: Ar ratio of 0.66:99.34 was found to be 0.43 MPa $m^{-1/2}$ and 1.41 MPa $m^{-1/2}$ respectively. The results show that fracture toughness of the Ti-B-N films increases with nitrogen incorporation. Thus, the Ti-B-N films can be tailored to obtain the optimal values of hardness and toughness. The XPS and other studies revealed the formation of TiN and soft h-BN phase [266]. Thus, the presence of h-BN enhances the toughness as soft phase in hard matrix compared to only TiB_2 Film. Nitrogen incorporation also affects the topography and grain size decreased with nitrogen content increase. The topographic picture of TiB_2 and TiBN is shown in Figure 21. Thus, from above it is clear that the nanocomposite Ti-B-N film showed a good enhancement of toughness compared to TiB_2 film.

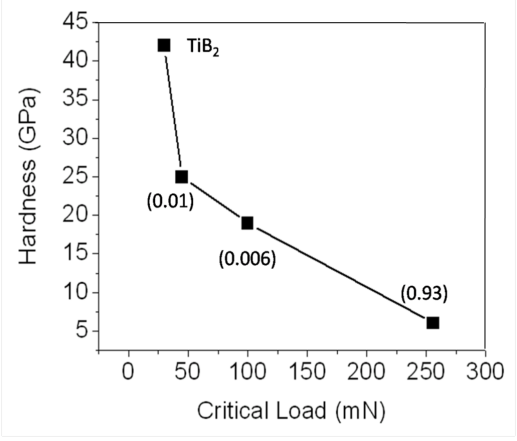

Figure 20: Hardness vs Critical load for the Ti-B-N films, the parenthesis shows the nitrogen fraction

9.2 Nanocomposite Ti-Si-B-C hard coating

The addition of elements such as C, N, Al, and Si can alter the properties of TiB_2. Ti-Si-B-C, adding suitably Si and C in TiB_2 have shown significant enhancement in different properties. The Magnetron sputtered TiSiBC film's properties can be tailored by suitable adjustments of deposi-

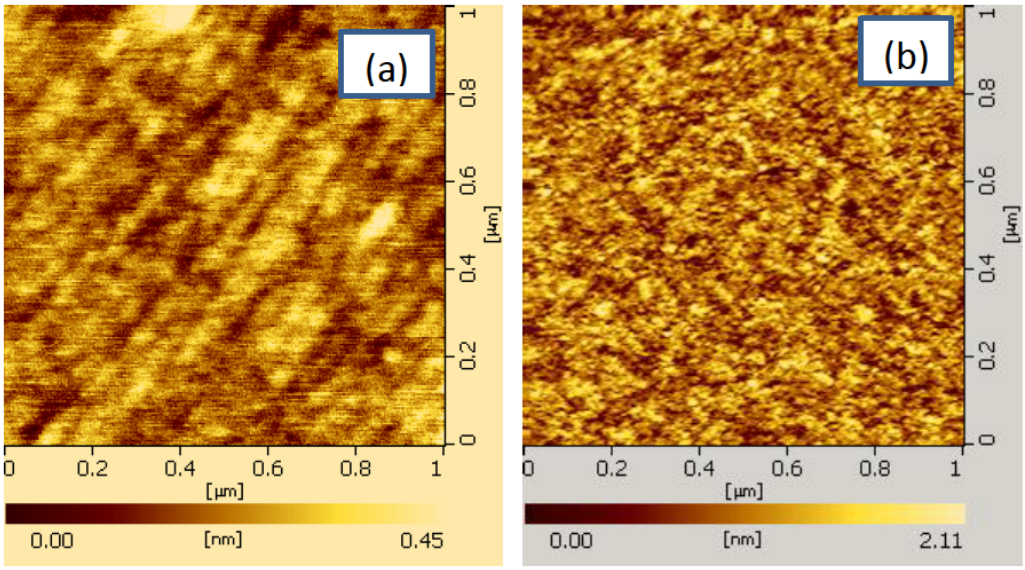

Figure 21: AFM micrographs of the deposited films (a) TiB2 (b) TiBN [267]

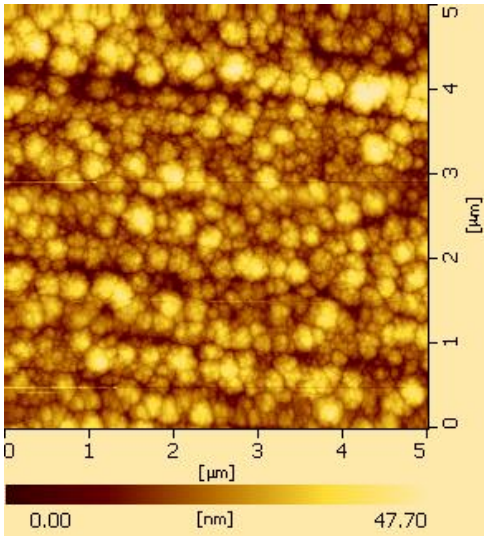

Figure 22: AFM Picture of TiSiBC hard coating deposited by Magnetron sputtering

tion parameter. The films are nanocomposite having very fine crystallites of the order of 5-10 nm and can be varied to 150 nm; accordingly the mechanical behavior also changes. The AFM and TEM pictures of nanocomposite TiSiBC thin films are shown in Figure 22 and 23. It consists of two crystalline phases TiB_2 and SiC in amorphous Ti-Si-B-C amorphous matrix. The crystalline particles were homogeneously dispersed in the matrix.

The hardness and modulus of the order of 45 GPa and 450 GPa with Percentage elastic recovery around 50% have been obtained. The H/E ratio was around 0.1, confirming them to be tough too. The immiscibility of the nanocrystalline phases and thermal segregation of nanocrystalline phase contributes for increase in hardness. The critical load (Lc) during scratch test was found to be about 21 N, and the coefficient of friction varied between 0.1-.2. The calculated average toughness measured by nanoindentation using cube corner indentor was around 4.5-5 $MPam^{1/2}$ [268], which is higher in single layer film with good hardness compared to TiN, TiC, TiAlN, TiCN and other materials [269, 270]. The incorporation of C and Si also enhanced the oxidation and further hardness and toughness [182, 271].

Hence, it was observed that by suitable incorporation of the species like N, C, Si in TiB_2 system during deposition makes the nanocomposite hard coatings and enhances the toughness of the nanocomposite coatings significantly.

10 Toughness and hardness enhancement of TiN nanocomposite coatings by adding of different elements

10.1 Ti-Al-N and Ti-Al-Si-N nanocomposite hard coatings

Titanium nitride (TiN) hard coatings enhances the lifetime of cutting tools [272]. However, TiN oxidizes in air at 500°C limiting applications in high-speed cutting process. The

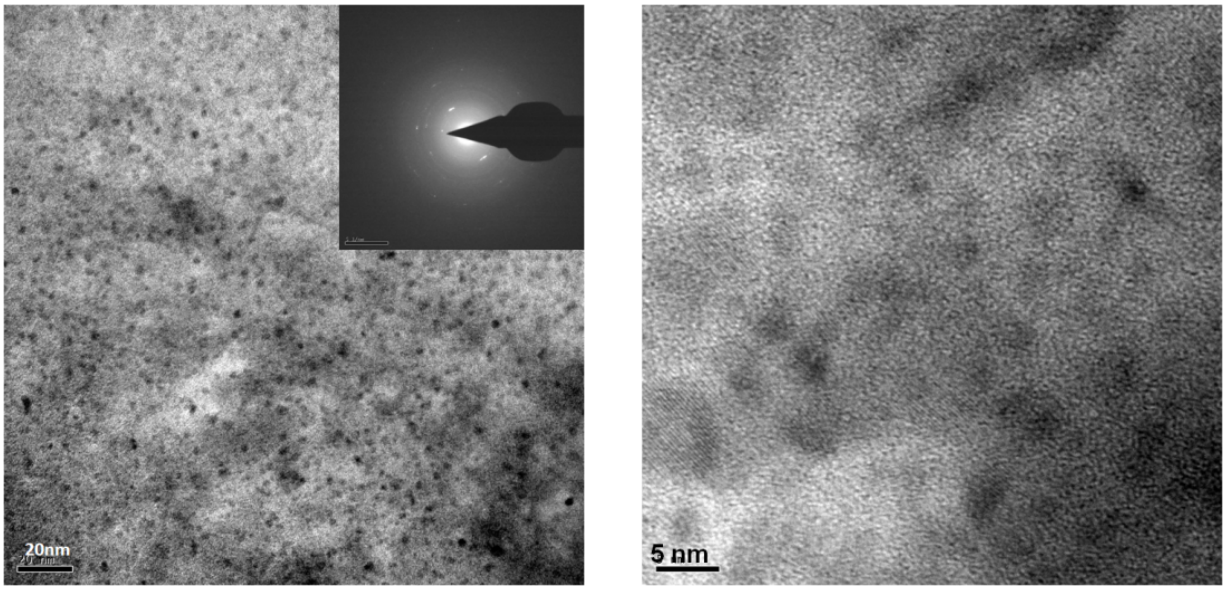

Figure 23: TEM Picture of TiSiBC hard coating deposited by Magnetron sputtering [268]

elements such as Al, Si, Cr or B into TiN are used to prepare nanocomposite coatings [273–276] to enhance the performance. At present, Si is the most frequently added element as it enhances the hardness and thermal stability [14, 277, 278]. Various techniques such as plasma-enhanced chemical vapor deposition (PECVD) [277–280], sputtering [281, 282], cathodic arc plasma evaporation [283, 284], and ion beam deposition [285] have been used to deposit TiAlSiN coatings. However, the PECVD process needs relatively higher substrate temperature hence, application of it is limited for precision components. The sputtered coatings have shown poor adhesion strength. Plasma immersion ion implantation and deposition (PIIID) have shown better adhesion strength and low temperature (t<200 °C) processing [286].

TiAlSiN coatings have TiN as crystalline phase mainly in amorphous matrix. The content of Al and Si when increased it has more nano crystal or amorphous structure respectively. The solubility of Al and Si is also observed in matrix [287, 288]. The hardness of the TiN film increases to 32 GPa from 19 GPa when Si content is incorporated around 0.9%. Further increase of Si content to 6.0% a very high hardness around 57 GPa is reported. However, at 15.7% it decreased to 28 GPa. The hardening mechanism for TiAlSiN coatings with different Si contents are solution hardening for lower Si content. Further increase of Si induces self-organized spinoidal phase segregation and the TiN grain is enveloped with thin amorphous Si_3N_4 layer that hinders the dislocation formation at the interface [14, 277, 279, 289, 290]. The decrease in hardness at higher *i.e.* 15.7% Si is due to increase of amorphous Si_3N_4 matrix phase that limits the grain boundary blocking effect [14]. The TiAlSiN film with the 6 mole % Si showed higher hardness, better toughness and adhesion strength.

In nc-TiN/a-Si_3N_4 hard nanocomposite, the grain refinement induced by Si_3N_4 increases the hardness; still dislocation movement within crystalline TiN phase can lead to deformation. The thin phase of silicon nitride around TiN crystallites interface inhibits deformation by grain boundary sliding. Nanocracks are deviated at grain boundaries leading to increase in toughness. The deformation process in such system is the propagation of nanocracks in the amorphous silicon nitride phase with the increase of a-Si_3N_4 phase and hardness decreases to that

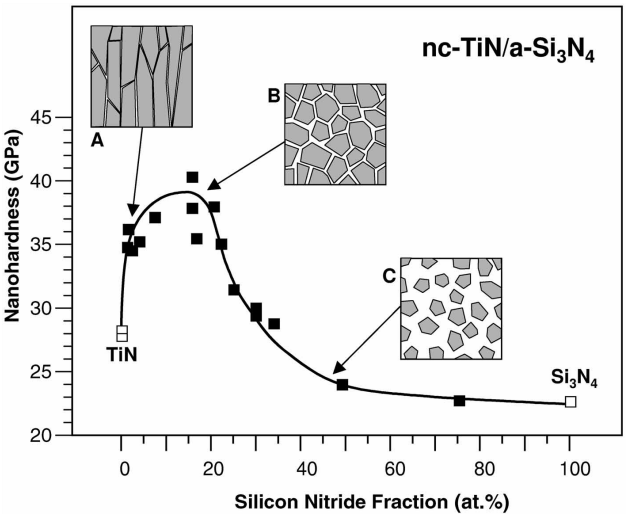

Figure 24: Hardness variation with Si % in Ti-Al-Si-N film [291].

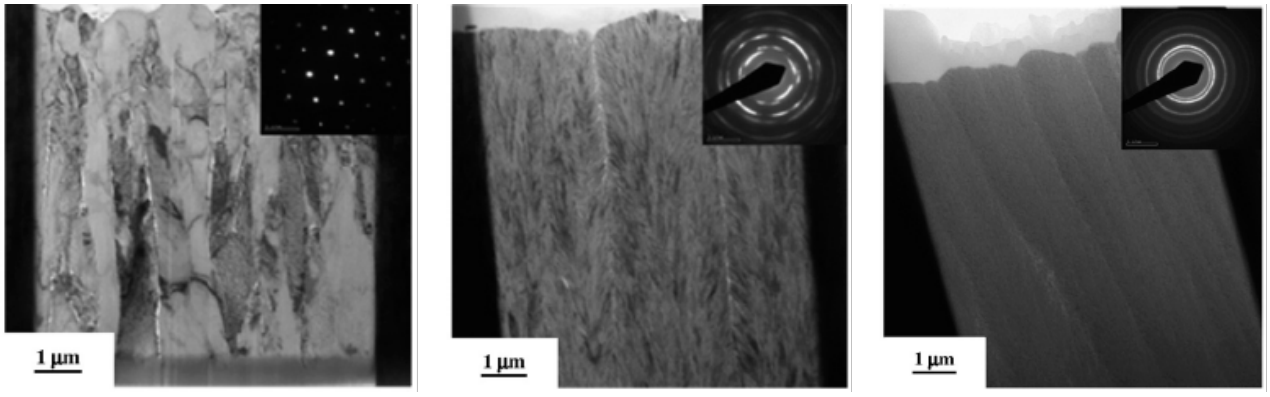

Figure 25: Cross sectional micrograph of with different percentages of Si a) TiN, b) Ti-Si-C-N16% c) Ti-Si-C-N 6% [302]

of silicon nitride. Figure 24 shows the hardness variation with Si content in Ti-Al-Si-N nanocomposite coating and the possible mechanism schematic of hardness at different percentages of Si [291]

10.2 Ti-Si-C-N nanocomposite hard coating

The addition of Si and C to TiN also enhanced the properties leading to nanocomposite hard and tough Ti–Si–C–N coatings [292–297]. The Ti–Si–C–N coating systems have been deposited by physical vapor deposition (PVD), magnetron sputtering [298–301] and chemical vapor deposition (CVD). Ti-Si-C-N nanocomposite coatings consist of nanocrystalline TiCN or TiN in silicon nitride amorphous matrix. The grain size was found to decrease from 20 nm to 6 nm with increase of Si content and grainboundary / amorphous area increased with Si. The addition of C further led to the decrease in crystalline particle size. The cross-section microstructure showed a coarse columnar structure for TiN, whereas with increase of Si content it showed very fine columnar structure and then featureless microstructure having very fine grains in amorphous matrix [Figure 25]. Hence, by the tailoring of microstructure dislocation movements gets restricted leading to increase in hardness and toughness. The hardness and the plastic deformation resistance, H^3/E^2 ratio [105, 302] were the function of (Si+C) concentration of coatings and both increased with the increase of (Si+C) content (Figure 26).

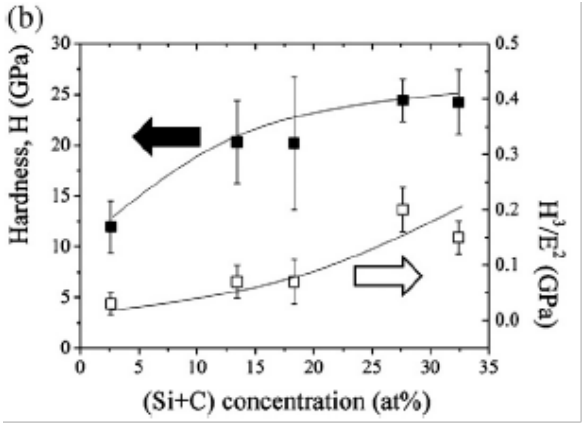

Figure 26: Hardness and H^3/E^2 variation with (Si +C) content in TiSiCN coating [302]

10.3 TiAlSiN nanocomposite coating having Ti-Al-N nanocomposite/ amorphous Si_3N_4 multilayer

As has been stated before the design of microstructure can change the hardness and toughness of the coatings. Nanocomposites having amorphous matrix with nanocrystalline grains enhances the toughness. This can also be further enhanced or by having multilayer of hard nanocomposite with amorphous layer composite coatings. In such combination a few nanometer thick amorphous layer can inhibit the dislocation generation and propagation. TiAlSiN coatings have been reported as layered coating with Ti-Al-N nanocomposite layer with Si_3N_4 alternate layer of thickness few nanometers. The backscattered image of such multilayer is shown in Figure 27 [303].

A maximum hardness of 35 GPa was obtained which is higher than monolayer film of TiAlSiN of same thickness. The dislocation motion is hindered due to under layer. The fracture mechanism changed from spalling to tensile cracking. The alternate layer with 20 nm periodic-

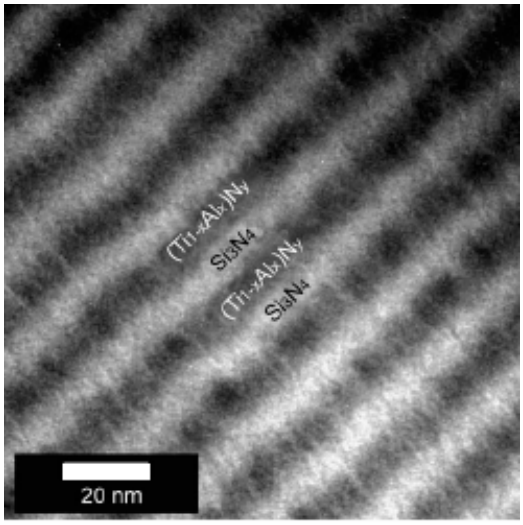

Figure 27: Ti-Al-Si-N multilayer coating having Ti-Al-N and Si_3N_4 alternate periodic layers [303]

ity showed nano cracks deflection at the internal interface and propagation in the interface (Figure 28) between the layers, suggesting such multilayers are tougher than single layer TiAlSiN or TiAlN. The critical load of scratch was found to increase to large extent. The dominant toughening mechanism was deflection of cracks between the layers and within the layers of nc-TiAlN /a-Si_3N_4 multilayer films.

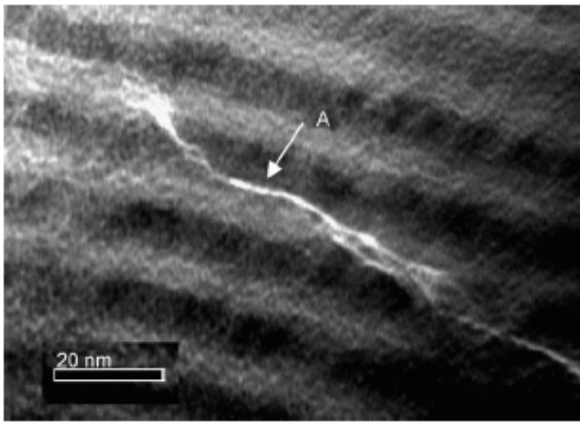

Figure 28: Ti-Al-Si-N coating with TiAlN/Si_3N_4 multilayer coating showing crack deflection at the interface and within the layer [303]

Hence, it was seen that by adding Si, C, Al to TiN the fracture toughness, hardness can be increased. The microstructure design is very important for achieving hardness and toughness in combination. Si and C addition and their ratio plays significant role in increasing hardness and toughness. The alternate layer of nanocomposite Ti-Al-N and amorphous silicon nitride layer enhance the toughness as compared to TiN coating, where the thickness of the periodic layer plays significant role in crack deflection and toughening mechanism.

Similarly, the AlCrN/TiSiN nanomultilayer coatings with single-phase solid solution structures have been reported recently and have shown a good toughness, H/E more than 0.1 along with hardness [304]

11 Al-Si-N nanocomposite hard coating

The ternary Al-Si-N nanocomposite coatings are less studied but are very potential material for electronic and optical application as well for wear protection coating for optical material as it has shown both optical visible range transparency along with high hardness and toughness. Si-doped AlN is considered as an interesting material for optoelectronic applications for field emission display, magneto optical disk and other applications. Nanocomposite coatings of nanocrystalline AlN embedded in an amorphous matrix of Si_3N_4 are hard and transparent and thus are useful as scratch-resistant optical coatings [305, 306]. Also, they have shown good oxidation resistance [307]. The reactive DC-magnetron sputtering (DCMS), chemical vapor deposition or reactive cathodic arc evaporation is used for the deposition of Al-Si-N nanocomposite coatings. Magnetron sputtering is one of the important processing methods for nanocomposite coatings; however, by addition of high power pulsed source in magnetron sputtering (HIPIMS) smoother morphology than normal DC source can be obtained. The H/E and the H^3/E^2 values are higher for the coatings deposited by pulsed source, and hence the tougher coatings [308]. Addition of Si also altered the hardness and toughness. Authors have also reported fabrication of optically transparent hard and tough coating by magnetron sputtering. The Al-Si-N nanocomposite film mainly consisted of AlN nanocrystallites in Al-Si-N matrix (Figure 29) [309]. The nitrogen partial pressure had the significant effect on the hardness and toughness [310]. The H/E value of were found to be of the order of 0.11 for Al-Si-N film having ratios Al:Si:N:: 57:32:11 in atom percent.

Hence, it was seen that like other systems discussed above the role of element addition such as Si is very significant to enhance the toughness and hardness of Al-Si-N system. The microstructure can be tailored by process parameter during deposition as well by compositions Si percentage in particular. There are other important systems also have been studied such as Zr-Si-N, Ti-Cr-Al-N, Zr-Cu-

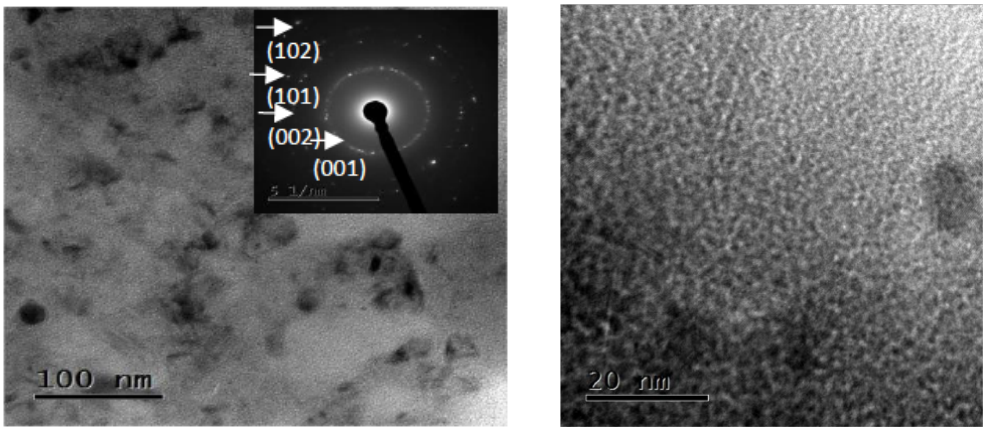

(a) (b)

Figure 29: TEM microstructure of Al-Si-N film showing (a) nanocrystallites in amorphous matrix (b) structure of matrix area [309]

N, Al-Cu-N, Zr-N etc [311–315] that also essentially depend on the microstructure design of the coating and hence the different additions of elements leading to enhanced toughness along with hardness.

Hence, in the nanocomposite hard coating systems to achieve the hardness along with good toughness it is established that films should have higher hardness with low E*, H/E* should be 0.1 or little and the elastic recovery be the order of 55-60%. The noncloumnar void free microstructure normally gives a higher tougher material compared to that of the columnar structure.

12 Issues and future directions in the area of nanocomposite hard coatings

The following issues and directions are very much required to be addressed further for the advancement and the application of the nanocomposite hard and tough coatings:

- The recovery, recrystallization, segregation, grain growth interdiffusion related phenomena are the controlling factor needs investigation in depth for the development of next generation nanocomposite coatings
- The nonlinear elastic behavior and mechanism of plastic deformation of nanocomposite coatings needs investigations.
- The elevated temperature and oxygen and other environment is very less. Such studies will help in designing the coatings for different industrial applications.
- It is important to understand and control the plastic instability of these materials; many nanocomposite coatings are macroscopically brittle but microscopically ductile.
- The process needs even more refinements to generate nanocomposite coating with controlled grain size, shape, crystallographic orientation and lattice structure.
- Understanding of deformation mechanisms in nanocrystalline multi-phase coating and better control of interface is still in infancy state.
- Measurement and methodology for estimating correct toughness by different methods and standard is still not there for nanocomposite coatings, needs development.
- Abinitio calculations on interfaces, multilayers and atomic scale simulations are almost not available, which needs to be developed for better understanding as well for less trial for processing of tailored nanocomposite coating.
- The control of interface states and understanding of non-equilibrium processes is still a change.
- Other than widely used sputtering and cathodic arc deposition, soft chemistry processes are very less available, which can meet the challenges.
- Stability is an issue for nanostructures, such studies are very few needs detailed investigations in many nanocomposite systems of coatings.
- During operation at higher temperatures, grain growth makes them conventional crystalline material thereby loosing the properties. Thermal stability

needs to be not only studied but newer high temperature stable at 1000^{o}C temperatures or higher coatings are required for different applications, such as high speed cutting tools, turbine blades for power industry and aerospace engine, nose-tip of high speed rockets and re-entry launches.

- Hard coatings with enhanced toughness resisting to cracking under an external loading are very less available. Optimum structure such as micro- and / or nano-structure of the coating having highest resistance to cracking is still not known.
- The interface of nanocrystalline and amorphous structure is less understood
- Residual stresses are less studied at different type of substrates
- There is lot of scattered data for similar system, needs a more effort so that a standard system can be obtained
- The toughness mechanism is still not clearly understood.
- Whether H/E*>0.1, high elastic recovery We, low effective Young's modulus E* are the sufficient conditions to form the hard coatings with enhanced toughness is not exactly answered yet.
- The understanding of charge transfer between nanograins with different chemical composition and different Fermi energies effecting functional properties are lacking.
- High-rate reactive deposition of hard coatings by PVD systems are required to be fabricated. New sputtering technologies based on strongly non-equilibrium at an atomic level are also required.
- Long-term durability tests for nanocomposite coatings are missing
- Very few coatings have been used on actual component such as cutting tools, piston etc. However, engine and component tests are required.
- Scale up of the coating for bigger components needs to be developed for successful coatings, along with cost and economics of it.

13 Summary

Thus, the present review focused on the enhancement of toughness in nanocomposite hard coatings, which is essentially required for to meet the complex demand of engineering applications. The importance of hard nanocomposite coatings, basic principles of hardening, methodology for the enhancement of toughness, processing of hard and tough nanocomposite coating have been explained. Some important systems such as Si-C-N, Si-C-N multilayers, Ti-B-N, Ti-Si-B-C, Ti-Si-N, Ti-Al-Si-N, Al-Si-N single layer nanocomposite and multilayer nanocomposite coatings have been discussed to emphasize the way of enhancement of toughness by microstructure modulations. Some of the other systems such as Ti-Cr-Al-N, Zr-Si-N etc were not discussed in detail but they also work on the similar line and are potential materials. It was seen that by Si, C, Al, N addition to TiN, TiB_2, AlN single phase materials enhances the fracture toughness, hardness and resilience due to formation of nanocomposite coatings. The microstructure design is very important for achieving hardness and toughness in combination. Si and C addition and their ratio plays significant role in increasing hardness and toughness. The alternate layer of nanocomposite and amorphous layer enhance the toughness, where the thickness of the periodic layer plays significant role in crack deflection and toughening mechanism. By suitable adjustment of different elements hardness, toughness and resilience of the coatings can be tailored to as per the requirement of the different engineering applications. The challenges of nanocomposite coatings, lack of understandings and future requirements are also discussed in the need for further research and Technology, requirements.

Acknowledgement: Author acknowledges the co researcher Dr. L.C. Pathak and her students namely Dr. A.S. Bhattacharyya, Dr. P.K.P Rupa, Mr. P. Mahato, Ms. Soni and other student who were working together before in carrying out different research work and for their degrees, which helped in writing this article. Author also acknowledges the other researchers for their publications in literature that helped to improve this article to great extent. Author also acknowledges the funding agencies of India that were received for different research work in nanocomposite hard coatings from CSIR and DST India.

References

[1] Anantharaman T. R, and C. Suryanarayan. Rapidly solidified metals: a technological overview. Acdermannsdorf, Switzerland: Trans Tech, 1987.

[2] Andres, R. P., R. S. Averback, W. L. Brown, L. E. Brus, W. A. Goddard, A. Kaldor *et al.* Research opportunities on clusters and cluster-assembled materials. *Journal of Materials Research*, Vol. 4, No. 3, 1989, pp. 704–736.

[3] Andrievski, R. A. Nanocrystalline high melting point compound-based materials. *Journal of Materials Science*, Vol. 29, No. 3. 1994, pp. 614-631.

[4] Armstrong, R. W., and T.N. Baker. Eds. *Yield, Flow and Fracture of Polycrystals*. Applied Science Pub., London, 1983.
[5] Suryanarayana, C. Structure and properties of nanocrystalline materials. *Bulletin of Materials Science*, Vol. 17, No. 4, 1994, pp. 307–346.
[6] Dobrzański, L. A., K. Lukaszkowicz, A. Zarychta, and L. Cunha. Corrosion resistance of multilayer coatings deposited by PVD techniques onto the brass substrate. *Journal of Materials Processing Technology*, Vol. 164–165, 2005, pp. 816–821.
[7] Lukaszkowicz, K., and L. A. Dobrzański. Structure and mechanical properties of gradient coatings deposited by PVD Technology, onto the X40CrMoV5-1 steel substrate. *Journal of Materials Science*, Vol. 43, No. 10, 2008, pp. 3400–3407.
[8] Matthews, A., and K. Holmberg. Coatings tribology: properties, techniques and applications in surface engineering. Elsevier, New York, 1994.
[9] Matthews, A., and D. Rickerby. Eds. Advanced Surface Coatings: a Handbook of Surface Engineering. Springer Netherlands, 1991.
[10] Riedel, R. Handbook of ceramic hard materials. Weinheim, New York: Wiley-VCH, 2000.
[11] Pogrebnyak, A. D., A. P. Shpak, V. M. Beresnev, G. V. Kirik, D. A. Kolesnikov, F. F. Komarov, *et al.* Stoichiometry, phase composition, and properties of superhard nanostructured Ti-Hf-Si-N coatings obtained by deposition from high-frequency vacuum-arc discharge. *Technical Physics Letters*, Vol. 37, No. 7, 2011, pp. 636–639.
[12] Veprek, S., H.D. Männling, P. Karvankova, and J. Prochazka. The issue of the reproducibility of deposition of superhard nanocomposites with hardness of ≥ 50 GPa. *Surface and Coatings Technology,* Vol. 200, No. 12–13, 2006, pp. 3876–3885.
[13] Mishra, S. K., C. Shekhar, P. K. P. Rupa, and L. C. Pathak. Effect of pressure and substrate temperature on the deposition of nano-structured silicon-carbon-nitride superhard coatings by magnetron sputtering. *Thin Solid Films*, Vol. 515, No. 11, 2007, pp. 4738–4744.
[14] Veprek, S., A. Niederhofer, K. Moto, T. Bolom, H. D. Männling, P. Nesladek, *et al.* Composition, nanostructure and origin of the ultrahardness in nc-TiN/a-Si3N4/a- and nc-TiSi2 nanocomposites with Hv = 80 to ≥ 105 GPa. *Surface and Coatings Technology,* Vol. 133–134, 2000, pp. 152–159.
[15] Zou, C.W., H. J. Wang, M. Li, Y. F. Yu, C. S. Liu, L. P. Guo, *et al.* Characterization and properties of TiN-containing amorphous Ti-Si-N nanocomposite coatings prepared by arc assisted middle frequency magnetron sputtering. *Vacuum*, Vol. 84, No. 6, 2010, pp. 817–822.
[16] Audronis, M., A. Leyland, P. J. Kelly, and A. Matthews. Composition and structure-property relationships of chromium-diboride/molybdenum-disulphide PVD nanocomposite hard coatings deposited by pulsed magnetron sputtering. *Applied Physics A: Materials Science and Processing*, Vol. 91, No. 1, 2008, pp. 77–86.
[17] Lukaszkowicz, K., J. Sondor, A. Kriz, and M. Pancielejko. Structure, mechanical properties and corrosion resistance of nanocomposite coatings deposited by PVD Technology, onto the X6CrNiMoTi17-12-2 and X40CrMoV5-1 steel substrates. *Journal of Materials Science*, Vol. 45, No. 6, 2010, pp. 1629–1637.
[18] Vaz, F., L. Rebouta, P. Goudeau, J. Pacaud, H. Garem, J. P. Rivière, *et al.* Characterization of $Ti_{1-x}Si_xN_y$ nanocomposite films. *Surface and Coatings Technology,* Vol. 133–134, 2000, pp. 307–313.
[19] Voevodin, A. A., and J. S. Zabinski. Nanocomposite and nanostructured tribological materials for space applications. *Composites Science and Technology*, Vol. 65, No. 5, 2005, pp. 741–748.
[20] Musil, J., and P. Zeman. Hard a-Si3N4/MeNx nanocomposite coatings with high thermal stability and high oxidation resistance. *Solid State Phenomena*, Vol. 127, 2007, pp. 31–36.
[21] Musil, J., J. Vlček, and P. Zeman, Hard amorphous nanocomposite coatings with oxidation resistance above 1000°C. *Advances in Applied Ceramics*, Vol. 107, No. 3, 2008, pp. 148–154.
[22] Cheng, Y. H., T. Browne, B. Heckerman, and E. I. Meletis, Mechanical and tribological properties of nanocomposite TiSiN coatings. *Surface and Coatings Technology,* Vol. 204, No. 14, 2010, pp. 2123–2129.
[23] Polychronopoulou, K., M. A. Baker, C. Rebholz, J. Neidhardt, M. O'Sullivan, A. E. Reiter, *et al.* The nanostructure, wear and corrosion performance of arc-evaporated CrBxNy nanocomposite coatings. *Surface and Coatings Technology,* Vol. 204, No. 3, 2009, pp. 246–255.
[24] Veprek, S., and M. J. G. Veprek-Heijman. Industrial applications of superhard nanocomposite coatings. *Surface and Coatings Technology,* Vol. 202, No. 21, 2008, pp. 5063–5073.
[25] Koch, C.C., I.A. Ovid'ko, S. Seal, and S. Veprek. Structural Nanocrystalline Materials, Fundamentals and Applications. Cambridge, UK: Cambridge University Press, 2007.
[26] Zhang, S., D. Sun, and X. L. Bui. Magnetron sputtered hard and yet tough nanocomposite coatings with case studies: Nanocrystalline TiN embedded in amorphous SiNx. In Nanocomposite thin films and coatings: processing, properties and performance, Zhang, S., and N. Ali, Eds., World Scientific, 2007.
[27] Musil, J. Hard nanocomposite coatings: Thermal stability, oxidation resistance and toughness. *Surface and Coatings Technology,* Vol. 207, 2012, pp. 50–65.
[28] Musil, J., and J. Vlček. Magnetron sputtering of hard nanocomposite coatings and their properties. *Surface and Coatings Technology,* Vol. 142–144, 2001, pp. 557–566.
[29] Pogrebnjak, A. D., and V. M. Beresnev. Hard Nanocomposite Coatings, Their Structure and Properties. In Nanocomposites - New Trends and Developments, Ebrahimi, F., Eds, BoD – Books on Demand, 2012.
[30] Holleck, H., and V. Schier. Multilayer PVD coatings for wear protection. *Surface and Coatings Technology,* Vol. 76–77, 1995, pp. 328–336.
[31] Wang,Y. X., S. Zhang, J. W. Lee, W. S. Lew, D. Sun, and B. Li, Hard yet tough ceramic coating: Not a dream any more-I. via nanostructured multilayering. *Nanoscience and Nanotechnology Letters*, Vol. 4, 2012, pp. 375–377.
[32] Dub, S., Y. Pauleau, and F. Thièry, Mechanical properties of nanostructured copper-hydrogenated amorphous carbon composite films studied by nanoindentation. *Surface and Coatings Technology,* Vol. 180–181, 2004, pp. 551–555.
[33] Palatnik, L. S., A. I. Il'mskii, and I. P. Sapelkin, Strength of multilayered vacuum condensates. *Physics of the Solid State*, Vol. 8, 1967, pp. 2016–2017.
[34] Palatnik, L. S., and A. I. Il'Inskii, Stabilization of high-strength vacuum-deposited films. *Doklady Physics*, Vol. 9, 1964, id. 93.
[35] Koehler, J. S. Attempt to Design a Strong Solid. *Physical Review B*, Vol. 2, 1970, pp. 547–551.
[36] Lehoczky, S. L. Strength enhancement in thin-layered Al-Cu laminates. *Journal of Applied Physics*, Vol. 49, No. 11, 1978, pp. 5479–5485.
[37] Springer, R. W., and D. S. Catlett. Structure and mechanical properties of Al/AlxOy vacuum- deposited laminates. *Thin Solid Films*,

Vol. 54, No. 2, 1978, pp. 197–205.
[38] Movchan, B. A., A. V. Demchishin, G. F. Badilenko, R. F. Bunshah, C. Sans, C. Deshpandey, *et al.* Structure-property relationships in microlaminate TiC/TiB2 condensates. *Thin Solid Films*, Vol. 97, No. 3, 1982, pp. 215–219.
[39] Kato, M., T. Mori, and L.H. Schwartz. Hardening by spinodal modulated structure. *Acta Metallurgica*, Vol. 38, No. 3, 1980, pp. 285–290.
[40] Holleck, H., and H. Schulz. Advanced layer material constitution. *Thin Solid Films*, Vol. 153, No. 1–3, 1987, pp. 11–17.
[41] Jankowski, A. F. Modelling the supermodulus effect in metallic multilayers. *Journal of Physics F: Metal Physics*, Vol. 18, No. 3, 1988, pp. 413–427.
[42] Shinn, M., L. Hultman, and S. A. Barnett. Growth, structure, and microhardness of epitaxial TiN/NbN superlattices. *Journal of Materials Research*, Vol. 7, No. 4, 1992, pp. 901–911.
[43] Sproul, W. D. Multilayer, multicomponent, and multiphase physical vapor deposition coatings for enhanced performance. *Journal of Vacuum Science & Technology A Vacuum Surfaces and Films*, Vol. 12, No. 4, 1994, pp. 1595–1601.
[44] Chu, X., and S. A. Barnett. Model of superlattice yield stress and hardness enhancements. *Journal of Applied Physics*, Vol. 77, No. 9, 1995, pp. 4403–4411.
[45] Robinson, P., A. Matthews, K. G. Swift, and S. Franklin. A computer knowledge-based system for surface coating and material selection. *Surface and Coatings Technology,* Vol. 62, No. 1–3, 1993, pp. 662–668.
[46] Voevodin, A. A., A. L. Erokhin, and V. V. Lyubimov. Formal Order for Search of the Principle Structure of Multilayer Coatings at Their Designing. *Physica Status Solidi*, Vol. 145, No. 2, 1994, pp. 565–574.
[47] Voevodin, A. A., S. D. Walck, and J. S. Zabinski. Architecture of multilayer nanocomposite coatings with super-hard diamondlike carbon layers for wear protection at high contact loads. *Wear*, Vol. 203–204, 1997, pp. 516–527.
[48] Vepřek. S, and S. Reiprich. A concept for the design of novel superhard coatings. *Thin Solid Films*, Vol. 268, No. 1–2, 1995, pp. 64–71.
[49] Vepřek, S. New development in superhard coatings: The superhard nanocrystalline-amorphous composites. *Thin Solid Films*, Vol. 317, No. 1–2, 1998, pp. 449–454.
[50] Vepřek, S. The search for novel, superhard materials. *Journal of Vacuum Science & Technology A Vacuum Surfaces and Films*, Vol. 17, No. 5, 1999, pp. 2401–2420.
[51] Veprek, S., and A. S. Argon. Towards the understanding of mechanical properties of super- and ultrahard nanocomposites. *Journal of Vacuum Science & Technology B: Microelectronics and Nanometer Structures*, Vol. 20, No. 2, 2002, id. 650.
[52] Musil, J., and J. Vlček. Magnetron sputtering of films with controlled texture and grain size. *Materials Chemistry and Physics*, Vol. 54, No. 1–3, 1998, pp. 116–122.
[53] Musil, J. Hard and superhard nanocomposite coatings *Surface and Coatings Technology,* Vol. 125, No. 1–3, 2000, pp. 322–330.
[54] Veprek, S., and A. S. Argon. Mechanical properties of superhard nanocomposites. *Surface and Coatings Technology,* Vol. 146–147, 2001, pp. 175–182.
[55] Dias, A., J. V. Breda, P. Moretto, J. Ordelman. Development of TiN-Si3N4 Nano composite coatings for wear resistance applications. Proceedings of the Tenth European Conference on Chemical Vapour Deposition. *Journal de Physique IV*, Vol. 5, 1995, pp. C5-831-C5-840.
[56] Musil, J., H. Jankovcova, and V. Cibulka. Formation of $Ti_{1-x}Si_x$ and $Ti_{1-x}Si_xN$ films by magnetron co-sputtering. *Czechoslovak Journal of Physics*, Vol. 49, No. 3, 1999, pp. 359–372.
[57] Vepřek, S. Conventional and new approaches towards the design of novel superhard materials. *Surface and Coatings Technology,* Vol. 97, No. 1–3, 1997, pp. 15–22.
[58] Mitterer, C., P. Losbichler, F. Hofer, P. Warbichler, P. N. Gibson, and W. Gissler. Nanocrystalline hard coatings within the quasi-binary system TiN-TiB2. *Vacuum*, Vol. 50, No. 3–4, 1998, pp. 313–318.
[59] Mitterer, C., P. H. Mayrhofer, M. Beschliesser, P. Losbichler, P. Warbichler, F. Hofer *et al.* Microstructure and properties of nanocomposite Ti-B-N and Ti-B-C coatings. *Surface and Coatings Technology,* Vol. 120–121, 1999, pp. 405–411.
[60] Irie, M., H. Ohara, A. Nakayama, N. Kitagawa, and T. Nomura. Deposition of Ni-TiN nano-composite films by cathodic arc ion-plating. *Nuclear Instruments and Methods in Physics Research Section B: Beam Interactions with Materials and Atoms*, Vol. 121, 1997, pp. 133–136.
[61] Musil, J., P. Zeman, H. Hrubý, and P. H. Mayrhofer. ZrN/Cu nanocomposite film - A novel superhard material. *Surface and Coatings Technology,* Vol. 120–121, 1999, pp. 179–183.
[62] Musil, J., and H. Poláková. Hard nanocomposite Zr-Y-N coatings, correlation between hardness and structure. *Surface and Coatings Technology,* Vol. 127, No. 1, 2000, pp. 99–106.
[63] Musil, J., and H. Hruby. Superhard nanocomposite $Ti_{1-x}Al_xN$ films prepared by magnetron sputtering. *Thin Solid Films*, Vol. 365, 2000, pp. 104–109.
[64] Benda, M., and J. Musil. Plasma nitriding enhanced by hollow cathode discharge - a new method for formation of superhard nanocomposite coatings on steel surfaces. *Vacuum*, Vol. 55, No. 2, 1999, pp. 171–175.
[65] Voevodin, A. A., S. V. Prasad, and J. S. Zabinski. Nanocrystalline carbide/amorphous carbon composites. *Journal of Applied Physics*, Vol. 82, No. 2, 1997, pp. 855–858.
[66] Ogletree, M. P. D., and O. R. Monteiro. Deposition of titanium carbide films from mixed carbon and titanium plasma streams. *Journal of Vacuum Science & Technology A Vacuum Surfaces and Films*, Vol. 15, No. 4, 1997, pp. 1943–1950.
[67] Voevodin, A. A., J. P. O'Neill, S. V. Prasad, and J. S. Zabinski. Nanocrystalline WC and WC/a-C composite coatings produced from intersected plasma fluxes at low deposition temperatures. *Journal of Vacuum Science & Technology A Vacuum Surfaces and Films*, Vol. 17, No. 3, 1999, pp. 986–992.
[68] Monteiro, O.R., M.P. Delplancke-Ogletree, R.Y. Lo, R. Winand, and I. Brown. Synthesis and characterization of thin films of WCx produced by mixing W and C plasma streams *Surface and Coatings Technology,* Vol. 94–95, 1997, pp. 220–225.
[69] Dieter, G. E. Mechanical Metallurgy. New York: McGrawHill, 1976.
[70] Marder, I., and J. Finberg. How things break. *Physics Today*, Vol. 49, 1996, pp. 24-29.
[71] Holleck, H.. Material selection for hard coatings. *Journal of Vacuum Science & Technology A Vacuum Surfaces and Films*, Vol. 4, No. 6, 1986, pp. 2661–2669.
[72] Voevodin, A. A., V. V Lyubimov, A. L. Yerokhin, and S. E. Spassky, Calculation of multilayer ion-plasma coating scheme. *Voprosy Atomnoy Nauki i Tekhniki*, Vol. 19, 1991, pp. 66–69.
[73] Lyubimov, V. V., A. A. Voevodin, S. E. Spassky, and A. L. Yerokhin. Stress analysis and failure possibility assessment of multilayer

physically vapour deposited coatings. *Thin Solid Films*, Vol. 207, No. 1–2, 1992, pp. 117–125.

[74] Fella, R., H. Holleck, and H. Schulz. Preparation and properties of WC-TiC-TiN gradient coatings. *Surface and Coatings Technology,* Vol. 36, No. 1–2, 1988, pp. 257–264.

[75] Monaghan, D. P., D. G. Teer, R. D. Arnell, I. Efeoglu, and W. Ahmed. Ion-assisted CVD of graded diamond like carbon (DLC) based coatings. Proceedings of the Ninth European Conference on Chemical Vapour Deposition. *Journal de Physique IV*, Vol. 3, No. 3, 1993, pp. 579–587.

[76] Voevodin, A. A., J. M. Schneider, C. Rebholz, and A. Matthews, Multilayer composite ceramic-metal-DLC coatings for sliding wear applications. *Tribology International*, Vol. 29, No. 7, 1996, pp. 559–570.

[77] Voevodin, A. A., M. A. Capano, S. J. P. Laube, M. S. Donley, and J. S. Zabinski. Design of a Ti/TiC/DLC functionally gradient coating based on studies of structural transitions in Ti-C thin films. *Thin Solid Films*, Vol. 298, No. 1–2, 1997, pp. 107–115.

[78] Lyubimov,V. V., A. A. Voevodin, A. L. Yerokhin, Y. S. Timofeev, and I. K. Arkhipov. Development and testing of multilayer physically vapour deposited coatings for piston rings. *Surface and Coatings Technology,* Vol. 52, No. 2, 1992, pp. 145–151.

[79] Voevodin, A. A., P. Stevenson, C. Rebholz, J. M. Schneider, and A. Matthews. Active process control of reactive sputter deposition. *Vacuum*, Vol. 46, No. 7, 1995, pp. 723–729.

[80] Mori, T., M. Noborisaka, T. Watanabe, and T. Suzuki. Oxidation resistance and hardness of TiAlSiN/CrAlYN multilayer films deposited by the arc ion plating method. *Surface and Coatings Technology,* Vol. 213, 2012, pp. 216–220.

[81] Zhang, Y., Y. Zhai, F. Li, S. Zhang, P. Zhang, and S. Zhang. Effect of microstructure and mechanical properties difference between sub-layers on the performance of alternate hard and soft diamond-like carbon multilayer films. *Surface and Coatings Technology,* Vol. 232, 2013, pp. 575–581.

[82] Qiang, L., B. Zhang, Y. Zhou, and J. Zhang. Improving the internal stress and wear resistance of DLC film by low content Ti doping. *Solid State Sciences*, Vol. 20, 2013, pp. 17–22.

[83] Zeman, H., J. Musil, and P. Zeman. Physical and mechanical properties of sputtered Ta–Si–N films with a high (≥ 40 at %) content of Si. *Journal of Vacuum Science & Technology A Vacuum Surfaces and Films*, Vol. 22, No. 3, 2004, id. 646.

[84] Karch, J., R. Birringer, and H. Gleiter. Ceramics ductile at low temperature. *Nature*, Vol. 330, No. 6148, 1987, pp. 556–558.

[85] Sherby, O. D., and J. Wadsworth. Superplasticity-Recent advances and future directions. *Progress in Materials Science*, Vol. 33, No. 3, 1989, pp. 169–221.

[86] Wakai, F. Superplasticity of ceramics. *Ceramics International*, Vol. 17, No. 3, 1991, pp. 153–163.

[87] Nieh, T. G., J. Wadsworth, and F. Wakai. Recent advances in superplastic ceramics and ceramic composites. *International Materials Reviews*, Vol. 36, No. 1, 1991, pp. 146–161.

[88] Langdon, T.G. The role of grain boundaries in high temperature deformation. *Materials Science and Engineering: A*, Vol. 166, No. 1–2, 1993, pp. 67–79.

[89] Koch, C.C., D.G. Morris, K. Lu, and A. Inoue. Ductility of nanostructured materials. *MRS Bulletin*, Vol. 24, No. 2, 1999, pp. 54–58.

[90] Siegel, R.W., G.E. Fougere. Grain size dependent mechanical properties in nanophase materials, Argonne National Lab, United States, 1995.

[91] Langdon, T.G. Significance of grain boundaries in the flow of polycrystalline materials. *Materials Science Forum*, Vol. 189–190, 1995, pp. 31–42.

[92] Sherby, D., O. G. Nieh, and J. Wadsworth. Some thoughts on future directions for research and applications in superplasticity. *Materials Science Forum*, Vol. 243–245, 1997, pp. 11–20.

[93] Schiøtz, J., F. D. Di Tolla, and K.W. Jacobsen. Softening of nanocrystalline metals at very small grain sizes. *Nature*, Vol. 391, No. 6667, 1998, pp. 561–563.

[94] Ma, S. L., D. Y. Ma, Y. Guo, B. Xu, G. Z. Wu, K. W. Xu, *et al.* Synthesis and characterization of super hard, self-lubricating Ti-Si-C-N nanocomposite coatings. *Acta Materialia*, Vol. 55, No. 18, 2007, pp. 6350–6355.

[95] Hao, S., B. Delley, S. Veprek, and C. Stampfl. Superhard nitride-based nanocomposites: Role of interfaces and effect of impurities. *Phys. Rev. Lett.*, Vol. 97, No. 8, 2006, pp. 1–4.

[96] Hao, S., B. Delley, and C. Stampfl. Structure and properties of TiN(111) Six Ny TiN(111) interfaces in superhard nanocomposites: First-principles investigations. *Physical Review B*, Vol. 74, No. 3, 2006, pp. 1–12.

[97] Matthews, A., R. Jones, and S. Dowey. Modelling the deformation behaviour of multilayer coatings. *Tribology Letters*, Vol. 11, No. 2, 2001, pp. 103–106.

[98] Münz, W. D., D. B. Lewis, P. E. Hovsepian, C. Schönjahn, A. Ehiasarian, and I. J. Smith. Industrial scale manufactured superlattice hard PVD coatings. *Surface Engineering*, Vol. 17, No. 1, 2001, pp. 15–27.

[99] Voevodin, A. A., and J. S. Zabinski. Load-adaptive crystalline-amorphous nanocomposites. *Journal of Materials Science*, Vol. 33, No. 2, 1998, pp. 319–327.

[100] Voevodin, A. A., and J. S. Zabinski. Supertough wear-resistant coatings with 'chameleon' surface adaptation. *Thin Solid Films*, Vol. 370, No. 1, 2000, pp. 223–231.

[101] Voevodin, A. A., J. J. Hu, J. G. Jones, T. A. Fitz, and J. S. Zabinski. Growth and structural characterization of yttria-stabilized zirconia-gold nanocomposite films with improved toughness. *Thin Solid Films*, Vol. 401, No. 1–2, 2001, pp. 187–195.

[102] Voevodin, A. A., J. S. Zabinski, and C. Muratore. Recent advances in hard, tough, and low friction nanocomposite coatings. *Tsinghua Science and Technology*, Vol. 10, No. 6, 2005, pp. 665–679.

[103] Mayrhofer, P. H., P. E. Hovsepian, C. Mitterer, and W. D. Münz. Calorimetric evidence for frictional self-adaptation of TiAlN/VN superlattice coatings. *Surface and Coatings Technology,* Vol. 177–178, 2004, pp. 341–347.

[104] Voevodin, A. A., J. P. O'Neill, and J. S. Zabinski. WC/DLC/WS2 nanocomposite coatings for aerospace tribology. *Tribology Letters*, Vol. 6, No. 2, 1999, pp. 75–78.

[105] Musil, J. Flexible hard nanocomposite coatings. *RSC Advances*, Vol. 5, No. 74, 2015, pp. 60482–60495.

[106] Bae, Y. W., W. Y. Lee, C. S. Yust, P. J. Blau, and T. M. Besmann. Synthesis and Friction Behavior of Chemically Vapor Deposited Composite Coatings Containing Discrete TiN and MoS2 Phases. *Journal of the American Ceramic Society*, Vol. 79, No. 4, 1996, pp. 819–824.

[107] Gilmore, R., M. A. Baker, P. N. Gibson, W. Gissler, M. Stoiber, P. Losbichler, *et al.* Low-friction TiN-MoS2 coatings produced by dc magnetron co-deposition. *Surface and Coatings Technology,* Vol. 108–109, No. 1–3, 1998, pp. 345–351.

[108] Gilmore, R., M. A. Baker, P. N. Gibson, and W. Gissler. Preparation and characterisation of low-friction TiB_2-based coatings by incorporation of C or MoS_2. *Surface and Coatings Technology,* Vol. 105, No. 1–2, 1998, pp. 45–50.

[109] Goller, R., P. Torri, M. A. Baker, R. Gilmore, and W. Gissler. The deposition of low-friction TiN-MoSx hard coatings by a combined arc evaporation and magnetron sputter process. *Surface and Coatings Technology,* Vol. 120–121, 1999, pp. 453–457.

[110] Voevodin, A. A., T. A. Fitz, J. J. Hu, and J. S. Zabinski, Nanocomposite tribological coatings with 'chameleon' surface adaptation. *Journal of Vacuum Science & Technology A Vacuum Surfaces and Films*, Vol. 20, No. 4, 2002, pp. 1434–1444.

[111] Xu, J., Z. Li, Z. H. Xie, P. Munroe, X. L. Lu, and X. F. Lan. Novel high damage-tolerant, wear resistant $MoSi_2$ -based nanocomposite coatings. *Applied Surface Science*, Vol. 270, 2013, pp. 418–427.

[112] Çalişkan, H., C. Kurbanoğlu, P. Panjan, M. Čekada, and D. Kramar. Wear behavior and cutting performance of nanostructured hard coatings on cemented carbide cutting tools in hard milling. *Tribology International*, Vol. 62, 2013, pp. 215–222.

[113] Ospina, R., D. Escobar-Rincón, P. J. Arango, E. Restrepo-Parra, and J. F. Jurado. Structural and chemical composition analysis of WCN produced by pulsed vacuum arc discharge. *Surface and Coatings Technology,* Vol. 232, 2013, pp. 96–100.

[114] Wu, L., X. Guo, and J. Zhang. Abrasive resistant coatings - A review. *Lubricants*, Vol. 2, No. 2, 2014, pp. 66–89.

[115] Prasad, S., and J. Zabinski. Super slippery solids. *Nature*, Vol. 387, No. 6635, 1997, pp. 761–763.

[116] Gardos, M. N. The synergistic effects of graphite on the friction and wear of MoS_2films in air. *Tribology Transactions*, Vol. 31, No. 2, pp. 1988, 214–224.

[117] Aouadi, S. M., Y. Paudel, B. Luster, S. Stadler, P. Kohli, C. Muratore, *et al.* Adaptive Mo 2N/MoS 2/Ag tribological nanocomposite coatings for aerospace applications. *Tribology Letters*, Vol. 29, No. 2, 2008, pp. 95–103.

[118] Czyzniewski, A., and W. Precht. Deposition and some properties of nanocrystalline, nanocomposite and amorphous carbon-based coatings for tribological applications. *Journal of Materials Processing Technology*, Vol. 157–158, 2004, pp. 274–283.

[119] Zhang, S., D. Sun, Y. Fu, and H. Du. Recent advances of superhard nanocomposite coatings: A review. *Surface and Coatings Technology,* Vol. 167, No. 2–3, pp. 2003, 113–119.

[120] Zhang, S., Y. Fu, H. Du, X. T. Zeng, and Y. C. Liu. Magnetron sputtering of nanocomposite (Ti, Cr)CN/DLC coatings. *Surface and Coatings Technology,* Vol. 162, No. 1, 2003, pp. 42–48.

[121] Fyta, M., C. Mathioudakis, I. N. Remediakis, and P. C. Kelires. Carbon-based nanostructured composite films: Elastic, mechanical and optoelectronic properties derived from computer simulations. *Surface and Coatings Technology,* Vol. 206, No. 4, 2011, pp. 696–702.

[122] Riedel, R., H. J. Kleebe, H. Schönfelder, and F. Aldinger. A covalent micro/nano-composite resistant to high-temperature oxidation. *Nature*, Vol. 374, No. 6522. 1995, pp. 526–528.

[123] Bill, J., J. Seitz, G. Thurn, J. Durr, J. Canel, B. Z. Janos, *et al.* Structure analysis and properties of Si-C-N ceramics derived from polysilazanes. *Physica Status Solidi (A)*, Vol. 166, No. 1, 1998, pp. 269–296.

[124] Saha, A., R. Raj, D. L. Williamson, and H. J. Kleebe. Characterization of nanodomains in polymer-derived SiCN ceramics employing multiple techniques. *Journal of the American Ceramic Society*, Vol. 88, No. 1, 2005, pp. 232–234.

[125] Gregori, G., H. J. Kleebe, H. Brequel, S. Enzo, and G. Ziegler, Microstructure evolution of precursors-derived SiCN ceramics upon thermal treatment between 1000 and 1400°C. *Journal of Non-Crystalline Solids*, Vol. 351, No. 16–17, 2005, pp. 1393–1402.

[126] Liew, L. A., R. A. Saravanan, V. M. Bright, M. L. Dunn, J. W. Daily, and R. Raj. Processing and characterization of silicon carbonnitride ceramics: Application of electrical properties towards MEMS thermal actuators. *Sensors and Actuators A: Physical*, Vol. 103, No. 1–2, 2003, pp. 171–181.

[127] Liew, L. A., W. Zhang, V. M. Bright, L. An, M. L. Dunn, and R. Raj. Fabrication of SiCN ceramic MEMS using injectable polymer-precursor technique. *Sensors and Actuators A: Physical*, Vol. 89, No. 1–2, 2001, pp. 64–70.

[128] Klaffke, D., R. Wäsche, N. Janakiraman, and F. Aldinger. Tribological characterisation of siliconcarbonitride ceramics derived from preceramic polymers. *Wear*, Vol. 260, No. 7–8, 2006, pp. 711–719.

[129] Liebau-Kunzmann, V., C. Fasel, R. Kolb, and R. Riedel. Lithium containing silazanes as precursors for SiCN: Li ceramics-A potential material for electrochemical applications. *Journal of the European Ceramic Society*, Vol. 26, No. 16, 2006, pp. 3897–3901.

[130] Shah, S. R., and R. Raj. Mechanical properties of a fully dense polymer derived ceramic made by a novel pressure casting process. *Acta Materialia*, Vol. 50, No. 16, 2002, pp. 4093–4103.

[131] Resta, N., C. Kohler, and H. R. Trebin. Molecular dynamics simulations of amorphous Si-C-N ceramics: Composition dependence of the atomic structure. *Journal of the American Ceramic Society*, Vol. 86, No. 8, 2003, pp. 1409–1414.

[132] Bauer, A., M. Christ, A. Zimmermann, and F. Aldinger. Fracture Toughness of Amorphous Precursor-Derived Ceramics in the Silicon-Carbon-Nitrogen System. *Journal of the American Ceramic Society*, Vol. 84, No. 10, 2001, pp. 2203–2207.

[133] Golczewski, J. A., and F. Aldinger, Thermodynamic modeling of amorphous Si-C-N ceramics derived from polymer precursors. *Journal of Non-Crystalline Solids*, Vol. 347, No. 1–3, 2004, pp. 204–210.

[134] Saha, A., S.R. Shah, and R. Raj, Amorphous silicon carbonitride fibers drawn from alkoxide modified ceraset^{TM}. *Journal of the American Ceramic Society*, Vol. 86, No. 8, 2003, pp. 1443–1445.

[135] Park, J. J., O. Komura, A. Yamakawa, and K. Niihara. Change of crystal phases and microstructure of amorphous Si-C-N powder by hot pressing. *Journal of the American Ceramic Society*, Vol. 81, No. 9, 1998, pp. 2253–2260.

[136] Friess, M., J. Bill, J. Golczewski, A. Zimmermann, F. Aldinger, R. Riedel, *et al.* "Crystallization of polymer-derived silicon carbonitride at 1873 K under nitrogen overpressure. *Journal of the American Ceramic Society*, Vol. 85, No. 10, 2002, pp. 2587–2589.

[137] Kleebe, H. J., D. Suttor, H. Müller, and G. Ziegler. Decomposition-crystallization of polymer-derived Si-C-N ceramics. *Journal of the American Ceramic Society*, Vol. 81, No. 11, 1998, pp. 2971–2977.

[138] Ferreira, I., E. Fortunato, P. Vilarinho, A.S. Viana, A.R. Ramos, E. Alves, *et al.* Hydrogenated silicon carbon nitride films obtained by HWCVD, PA-HWCVD and PECVD techniques. *Journal of Non-Crystalline Solids*, Vol. 352, No. 9-20, 2006, pp. 1361–1366.

[139] Zhang, D. H., L. Y. Yang, C. Y. Li, P. W. Lu, and P. D. Foo. Ta/SiCN bilayer barrier for Cu-ultra low k integration *Thin Solid Films*, Vol. 504, No. 1–2, 2006, pp. 235–238.

[140] Yang, L. Y., D. H. Zhang, C. Y. Li, R. Liu, P. W. Lu, P. D. Foo *et al.* Comparative investigation of TaN and SiCN barrier layer for Cu/ultra low k integration. *Thin Solid Films*, Vol. 504, No. 1–2,

2006, pp. 265–268.
[141] Li, X., S. Yang, and X. Wu. Preparation of silicon carbide nitride films on Si substrate by pulsed high-energy density plasma. *Journal of University of Science and Technology Beijing, Mineral, Metallurgy, Material*, Vol. 13, No. 3, 2006, pp. 272–276.
[142] Gao, Y., J. Wei, D. H. Zhang, Z. Q. Mo, P. Hing, and X. Shi. Effects of nitrogen fraction on the structure of amorphous silicon-carbon-nitrogen alloys. *Thin Solid Films*, Vol. 377–378, 2000, pp. 562–566.
[143] Ng,V. M., M. Xu, S. Y. Huang, J. D. Long, and S. Xu. Assembly and photoluminescence of SiCN nanoparticles. *Thin Solid Films*, Vol. 506–507, 2006, pp. 283–287.
[144] Yan, X. B., B. K. Tay, G. Chen, and S. R. Yang. Synthesis of silicon carbide nitride nanocomposite films by a simple electrochemical method. *Electrochemistry Communications*, Vol. 8, No. 5, 2006, pp. 737–740.
[145] Izumi, A., and K. Oda. Deposition of SiCN films using organic liquid materials by HWCVD method. *Thin Solid Films*, Vol. 501, No. 1–2, 2006, pp. 195–197.
[146] Fernández-Ramos, C., J. C. Sánchez-López, T. C. Rojas, and A. Fernández. Structural modifications of silicon-doped carbon nitride films during post-deposition annealing. *Diamond and Related Materials*, Vol. 12, No. 3–7, 2003, pp. 1055–1060.
[147] Nakaaki, I., and N. Saito. Optical, electrical and structural properties of amorphous SiCN:H films prepared by rf glow-discharge decomposition. *Applied Surface Science*, Vol. 169–170, 2001, pp. 468–471.
[148] Chen, C. W., C. C. Huang, Y. Y. Lin, L. C. Chen, K. H. Chen, and W. F. Su. Optical properties and photoconductivity of amorphous silicon carbon nitride thin film and its application for UV detection. *Diamond and Related Materials*, Vol. 14, No. 3–7, 2005, pp. 1010–1013.
[149] Chen, C. W., C. C. Huang, Y. Y. Lin, L. C. Chen, and K. H. Chen. The affinity of Si-N and Si-C bonding in amorphous silicon carbon nitride (a-SiCN) thin film. *Diamond and Related Materials*, Vol. 14, No. 3–7, 2005, pp. 1126–1130.
[150] Smirnova, T. P., A. M. Badalian, L. V. Yakovkina, V. V. Kaichev, V. I. Bukhtiyarov, A. N. Shmakov *et al.*, SiCN alloys obtained by remote plasma chemical vapour deposition from novel precursors. *Thin Solid Films*, Vol. 429, No. 1–2, 2003, pp. 144–151.
[151] Chen, C. W., P. T. Liu, T. C. Chang, J. H. Yang, T. M. Tsai, H. H. Wu, *et al.* Cu-penetration induced breakdown mechanism for a-SiCN. *Thin Solid Films*, Vol. 469–470, 2004, pp. 388–392.
[152] Jedrzejowski, P., J. E. Klemberg-Sapieha, and L. Martinu. Quaternary hard nanocomposite TiCxNy/SiCN coatings prepared by plasma enhanced chemical vapor deposition. *Thin Solid Films*, Vol. 466, No. 1–2, 2004, pp. 189–196.
[153] Cheng, W., J. Jiang, Y. Zhang, H. Zhu, and D. Shen. Effect of the deposition conditions on the morphology and bonding structure of SiCN films. *Materials Chemistry and Physics,* Vol. 85, No. 2–3, 2004, pp. 370–376.
[154] Jedrzejowski, P., J. Cizek, A. Amassian, J. E. Klemberg-Sapieha, J. Vlcek, and L. Martinu. Mechanical and optical properties of hard SiCN coatings prepared by PECVD, *Thin Solid Films*, vol. 447–448, 2004,pp. 201–207.
[155] Chen, C. W., T. C. Chang, P. T. Liu, T. M. Tsai, H. C. Huang, J. M. Chen, *et al.* Investigation of the electrical properties and reliability of amorphous SiCN. *Thin Solid Films*, Vol. 447–448, 2004, pp. 632–637.
[156] Xie, E., Z. Ma, H. Lin, Z. Zhang, and D. He. Preparation and characterization of SiCN films. *Optical Materials*, Vol. 23, No. 1–2, 2003, pp. 151–156.
[157] Matsutani, T., T. Asanuma, C. Liu, M. Kiuchi, and T. Takeuchi. Ion beam-induced chemical vapor deposition with hexamethyldisilane for hydrogenated amorphous silicon carbide and silicon carbonitride films. *Surface and Coatings Technology,* Vol. 169–170, 2003, pp. 624–627.
[158] Barreca, F., E. Fazio, F. Neri, and S. Trusso. Electronic properties of PLD prepared nitrogenated a-SiC thin films. *Thin Solid Films*, Vol. 433, No. 1-2, 2003, pp. 34–38.
[159] Lin, H. Y., Y. C. Chen, C. Y. Lin, Y. P. Tong, L. G. Hwa, K. H. Chen, *et al.* Field emission of nanostructured amorphous SiCN films deposited by reactive magnetron sputtering of SiC in CH4/N2 atmosphere. *Thin Solid Films*, Vol. 416, No. 1–2, 2002, pp. 85–91.
[160] Mitu, B., G. Dinescu, E. Budianu, A. Ferrari, M. Balucani, G. Lamedica, *et al.* Formation of intermediate SiCN interlayer during deposition of CN x on a-Si:H or a-SiC:H thin films. *Applied Surface Science*, Vol. 184, No. 1–4, 2001, pp. 96–100.
[161] Wu, J. J., K. H. Chen, C. Y. Wen, L. C. Chen, Y. -C. Yu, C. -W. Wang, *et al.* Effect of dilution gas on SiCN films growth using methylamine. *Materials Chemistry and Physics*, Vol. 72, No. 2, 2001, pp. 240–244.
[162] Zhang, D. H., Y. Gao, J. Wei, and Z. Q. Mo. Influence of silane partial pressure on the properties of amorphous SiCN films prepared by ECR-CVD. *Thin Solid Films*, Vol. 377–378, 2000, pp. 607–610.
[163] Sundaram, K. B., and J. Alizadeh. Deposition and optical studies of silicon carbide nitride thin films. *Thin Solid Films*, Vol. 370, No. 1, 2000, pp. 151–154.
[164] Wu, J. J., K. H. Chen, C. Y. Wen, L. C. Chen, X. -J. Guo, H. J. Lo, *et al.* Effect of carbon sources on silicon carbon nitride films growth in an electron cyclotron resonance plasma chemical vapor deposition reactor. *Diamond and Related Materials*, Vol. 9, 2000, pp. 556–561.
[165] Xiao, X. C., Y. W. Li, L. X. Song, X. F. Peng, and X. F. Hu. Structural analysis and microstructural observation of SiC x N y films prepared by reactive sputtering of SiC in N 2 and Ar. *Applied Surface Science*, Vol. 156, No. 1–4, 2000, pp. 155–160.
[166] Wu, J. J., C. -T. Wu, Y. -C. Liao, T. -R. Lu, L. C. Chen, K. H. Chen, *et al.* Deposition of silicon carbon nitride films by ion beam sputtering *Thin Solid Films*, Vol. 355, 1999, pp. 417–422.
[167] Kato, M., J. Zheng, S. Takezoe, and K. Nakasa. Evaluation of wear resistance of sputtered amorphous SiCN film and measurement of delamination strength of film by micro edge-indent method delamination strength of film by micro edge-indent method. *Journal of the Society of Materials Science*, Japan, Vol. 54, 2005, p. 1022.
[168] Mishra, S. K. Nano and nanocomposite superhard coatings of silicon carbonitride and titanium diboride by magnetron Sputtering. *International Journal of Applied Ceramic Technology*, Vol. 6, No. 3, 2009, pp. 345–354.
[169] Bhattachryya, A. S., S. Mukherjee, S. K. Mishra. The effects of substrate temperature on the microstructure of thin film Si-C-N coatings deposited by RF magnetron sputtering. *European Coatings Journal*, Vol. 3, 2009, pp. 108–114.
[170] Bhattacharyya, A. S., G. C. Das, S. Mukherjee, and S.K. Mishra. Effect of radio frequency and direct current modes of deposition on protective metallurgical hard silicon carbon nitride coatings by magnetron sputtering. *Vacuum*, Vol. 83, No. 12, 2009, pp. 1464–1469.

[171] Mishra, S. K., and A. S. Bhattacharyya. Effect of substrate temperature on the adhesion properties of magnetron sputtered nano-composite Si-C-N hard thin films. *Materials Letters*, Vol. 62, No. 3, 2008, pp. 398–402.

[172] Burnett, P. J., and D. S. Rickerby. The scratch adhesion test: An elastic-plastic indentation analysis. *Thin Solid Films*, Vol. 157, No. 2, 1988, pp. 233–254.

[173] Dyrda, K., and M. Sayer. Critical loads and effective frictional force measurements in the industrial scratch testing of TiN on M2 tool steel. *Thin Solid Films*, Vol. 355, 1999, pp. 277–283.

[174] Mehrotra, P. K., and D. T. Quinto. Techniques for evaluating mechanical properties of hard coatings. *Journal of Vacuum Science & Technology A Vacuum Surfaces and Films*, Vol. 3, No. 6, 1985, pp. 2401–2405.

[175] Bull, S. J., and E. G. Berasetegui. An overview of the potential of quantitative coating adhesion measurement by scratch testing. *Tribology International*, Vol. 39, No. 2, 2006, pp. 99–114.

[176] Bhattacharyya, A. S., S. K. Mishra, and S. Mukherjee. Correlation of structure and hardness of rf magnetron sputtered silicon carbonitride films. *Journal of Vacuum Science & Technology A Vacuum Surfaces and Films*, Vol. 28, No. 4, 2010, pp. 505–509.

[177] Bhushan, B., and X. Li. Nanomechanical characterisation of solid surfaces and thin films. *International Materials Reviews*, Vol. 48, No. 3, 2003, pp. 125–164.

[178] Bhattacharyya, A. S., and S.K. Mishra. Micro/nanomechanical behavior of magnetron sputtered Si-C-N coatings through nanoindentation and scratch tests. *Journal of Micromechanics and Microengineering*, Vol. 21, No. 1, 2011, id. 015011.

[179] Bhattacharyya, A. S., S. K. Mishra, S. Mukherjee, and G. C. Das. A comparative study of Si-C-N films on different substrates grown by RF magnetron sputtering. *Journal of Alloys and Compounds*, Vol. 478, No. 1–2, 2009, pp. 474–478.

[180] Wang, E. G. Research on Carbon Nitrides. *Progress in Materials Science*, Vol. 41, No. 5, 1997, pp. 241–298.

[181] Leyland, A., and A. Matthews, On the significance of the H/E ratio in wear control: A nanocomposite coating approach to optimised tribological behaviour. *Wear*, Vol. 246, No. 1–2, 2000, pp. 1–11.

[182] Ding, J., Y. Meng, and S. Wen. Mechanical properties and fracture toughness of multilayer hard coatings using nanoindentation. *Thin Solid Films*, Vol. 371, No. 1, 2000, pp. 178–182.

[183] Mishra, S. K., D. Verma, S. Bysakh, and L. C. Pathak. Hard and soft multilayered SiCN nanocoatings with high hardness and toughness. *Journal of Nanomaterials*, 2013.

[184] Musil, J., J. Sklenka, and J. Prochazka. Protective over-layer coating preventing cracking of thin films deposited on flexible substrates. *Surface and Coatings Technology,* Vol. 240, 2014, pp. 275–280.

[185] Munro, R. G. Material Properties of Titanium Diboride. *Journal of Research of the National Institute of Standards and Technology*, Vol. 105, No. 5, 2000, pp. 709–720.

[186] Berger, M., M. Larsson, and S. Hogmark. Evaluation of magnetron-sputtered TiB2 intended for tribological applications. *Surface and Coatings Technology,* Vol. 124, No. 2–3, 2000, pp. 253–261.

[187] Choi, C. S., G. C. Xing, G. A. Ruggles, and C. M. Osburn. The effect of annealing on resistivity of low pressure chemical vapor deposited titanium diboride. *Journal of Applied Physics*, Vol. 69, No. 11, 1991, pp. 7853–7861.

[188] Voss, L., R. Khanna, S. J. Pearton, F. Ren, and I. I. Kravchenko. Use of TiB 2 diffusion barriers for Ni/Au ohmic contacts on p-GaN. *Applied Surface Science*, Vol. 253, No. 3, 2006, pp. 1255–1259.

[189] Schultes, G., M. Schmitt, D. Goettel, and O. Freitag-Weber. Strain sensitivity of TiB2, TiSi2, TaSi2 and WSi2 thin films as possible candidates for high temperature strain gauges. *Sensors and Actuators A: Physical*, Vol. 126, No. 2, 2006, pp. 287–291.

[190] Kaminsky, M., R. Nielsen, and P. Zschack. Preferential sputtering of TiC and TiB2 coatings under D+ and 4He+ bombardment: Partial yields. *Journal of Vacuum Science and Technology*, Vol. 20, No. 4, 1981, pp. 1304–1308.

[191] Doyle, B. L., and F. L. Vook. Hydrogen retention and release in first-wall coatings for tokamaks. *Thin Solid Films*, Vol. 63, No. 2, 1979, pp. 277–281.

[192] Pfohl, C., A. Bulak, and K. T. Rie. Development of titanium diboride coatings deposited by PACVD. *Surface and Coatings Technology,* Vol. 131, No. 1–3, 2000, pp. 141–146.

[193] Haubner, R.,The history of hard CVD coatings for tool applications at the University of Technology, Vienna. *International Journal of Refractory Metals and Hard Materials*, Vol. 41, 2013, pp. 22–34.

[194] Pfohl, C., and K.T. Rie. Wear-resistant PACVD coatings of the system Ti-B-N. *Surface and Coatings Technology,* Vol. 116–119, 1999, pp. 911–915.

[195] Lee, S. H., K. H. Nam, S. C. Hong, and J. J. Lee. Low temperature deposition of TiB2 by inductively coupled plasma assisted CVD. *Surface and Coatings Technology,* Vol. 201, No. 9-11, 2007, pp. 5211–5215.

[196] Williams, L. M. Plasma enhanced chemical vapor deposition of titanium diboride films. *Applied Physics Letters*, Vol. 46, No. 1, 1985, pp. 43–45.

[197] Beckloff, B. N., and W.J. Lackey. Process-structure-reflectance correlations for TiB2 films prepared by chemical vapor deposition. *Journal of the American Ceramic Society*, Vol. 82, No. 3, 1999, pp. 503–512.

[198] Motojima, S., and R. Azuma. Chemical vapour deposition of TiB2 protective layers on a brass plate. *Journal of Materials Science*, Vol. 23, No. 12, 1988, pp. 4375–4378.

[199] Becht, J. G. M., P. J. Van Der Put, and J. Schoonman. CVD of laminar composites in the system TiN-TiB2. *Solid State Ionics*, Vol. 32–33, 1989, pp. 789–794.

[200] Caputo, A. J., W. J. Lackey, I. G. Wright, and P. Angelini. Chemical vapor deposition of erosion-resistant TiB2 coatings. *Journal of the Electrochemical Society*, Vol. 132, 1985, p. 2274.

[201] Besmann, T. M., and K. E. Spear. Morphology of chemical vapor deposited titanium diboride. *Vap. Growth Ep.*, 1975, pp. 60–65.

[202] Pierson, H. O., E. Randich, and D. M. Mattox. The chemical vapor deposition of TiB_2 on graphite. *Journal of the Less Common Metals*, Vol. 67, No. 2, 1979, pp. 381–388.

[203] Takahashi, T., and H. Itoh. Ultrasonic chemical vapor deposition of TiB2 thick films. *Journal of Crystal Growth*, Vol. 49, No. 3, 1980, pp. 445–450.

[204] Pierson, H. O., and A. W. Mullendore, The chemical vapor deposition of TiB_2 from diborane. *Thin Solid Films*, Vol. 72, No. 3, 1980, pp. 511–516.

[205] Kumar, N., Y. Yang, W. Noh, G. S. Girolami, and J. R. Abelson. Titanium diboride thin films by low-temperature chemical vapor deposition from the single source precursor Ti(BH 4) 3(1,2-dimethoxyethane). *Chemistry of Materials*, Vol. 19, No. 15, 2007, pp. 3802–3807.

[206] Ferrando, V., D. Marré, P. Manfrinetti, I. Pallecchi, C. Tarantini, and C. Ferdeghini. Pulsed laser deposition of epitaxial titanium diboride thin films. *Thin Solid Films*, Vol. 444, No. 1–2, 2003, pp. 91–94.

[207] Zhai, H. Y., H. M. Christen, C. Cantoni, A. Goyal, and D. H. Lowndes. Epitaxial titanium diboride films grown by pulsed-laser deposition. *Applied Physics Letters*, Vol. 80, No. 11, 2002, pp. 1963–1965.

[208] Zergioti, I., C. Fotakis, and G. N. Haidemenopoulos. Growth of TiB_2 and TiC coatings using pulsed laser deposition. *Thin Solid Films*, Vol. 303, No. 1–2, 1997, pp. 39–46.

[209] Rivière, J. P., S. Miguet, M. Cahoreau, J. Chaumont, and J. Delafond. Formation of TiB_2 coatings at room temperature by dynamic ion mixing. *Surface and Coatings Technology,* Vol. 84, No. 1–3, 1996, pp. 398–403.

[210] Panich, N., and Y. Sun. Mechanical properties of TiB2-based nanostructured coatings. *Surface and Coatings Technology,* Vol. 198, No. 1-3, 2005, pp. 14–19.

[211] Prakash, B., C. Ftikos, and J. P. Celis. Fretting wear behavior of PVD TiB2 coatings. *Surface and Coatings Technology,* Vol. 154, No. 2–3, 2002, pp. 182–188.

[212] Chen, J., and J. A. Barnard. Growth , structure and stress of sputtered TiB_2 thin films. *Materials Science and Engineering: A*, Vol. 191, 1995, pp. 233–238.

[213] Berger, M., E. Coronel, and E. Olsson. Microstructure of d.c. magnetron sputtered TiB2 coatings. *Surface and Coatings Technology,* Vol. 185, No. 2–3, 2004, pp. 240–244.

[214] Berger, M., L. Karlsson, M. Larsson, and S. Hogmark. Low stress TiB2 coatings with improved tribological properties. *Thin Solid Films*, Vol. 401, No. 1–2, 2001, pp. 179–186.

[215] Kunc, F., J. Musil, P. H. Mayrhofer, and C. Mitterer. Low-stress superhard Ti–B films prepared by magnetron sputtering. *Surface and Coatings Technology,* Vol. 174 – 175, 2003, pp. 744–753.

[216] Kelesoglu, E., and C. Mitterer. Structure and properties of TiB2 based coatings prepared by unbalanced DC magnetron sputtering. *Surface and Coatings Technology,* Vol. 98, No. 1–3, 1998, pp. 1483–1489.

[217] Larsson, T., H. O. Blom, S. Berg, and M. Östling. Reactive sputtering of titanium boride. *Thin Solid Films*, Vol. 172, No. 1, 1989, pp. 133–140.

[218] Yoshisawa, I., R. Urao, Y. Hori, K. Akaishi, and K. Kamada. Characterization of TiB2 coated layer by X-Ray lattice constant measurement. *Journal of Nuclear Materials*, Vol. 103, 1981, pp. 267–272.

[219] Sanchez, C. M. T., B. R. Plata, M. E. H. M. da Costa, and F. L. Freire Jr. Titanium diboride thin films produced by dc-magnetron sputtering: Structural and mechanical properties. *Surface and Coatings Technology,* Vol. 205, No. 12, 2011, pp. 3698–3702.

[220] Wong, M. S., and Y. C. Lee. Deposition and characterization of Ti-B-N monolithic and multilayer coatings. *Surface and Coatings Technology,* Vol. 120–121, 1999, pp. 194–199.

[221] Panich, N., and Y. Sun, Effect of substrate rotation on structure, hardness and adhesion of magnetron sputtered TiB2 coating on high speed steel. *Thin Solid Films*, Vol. 500, No. 1–2, 2006, pp. 190–196.

[222] Broszeit, E., B. Matthes, W. Herr, and K. H. Kloos. Tribological properties of r.f. sputtered Ti-B-N coatings under various pin-on-disc wear test conditions. *Surface and Coatings Technology,* Vol. 58, No. 1, 1993, pp. 29–35.

[223] Shikama, T., Y. Sakai, M. Fukutomi, and M. Okada. Deposition of TiB_2 films by a co-sputtering method, *Thin Solid Films*, Vol. 156, No. 2, 1988, pp. 287–294.

[224] Knotek, O., and F. Löffler. Superhard physical vapour deposition coatings in the Ti-B-C-N system. *Journal of Hard Materials*, Vol. 3, 1992, pp. 29–38,.

[225] Treglio, J. R., S. Trujillo, and A. J. Perry. Deposition of TiB2 at low temperature with low residual stress by a vacuum arc plasma source. *Surface and Coatings Technology,* Vol. 61, No. 1–3, 1993, pp. 315–319.

[226] Gissler, W. Structure and properties of Ti — B — N coatings. *Surface and Coatings Technology,* Vol. 68/69, 1994, pp. 556–563.

[227] Herr, W., B. Matthes, E. Broszeit, and K. H. Kloos. Fundamental properties and wear resistance of r.f.-sputtered TiB_2 and Ti(B,N) coatings. *Materials Science and Engineering: A*, Vol. 140, 1991, pp. 616–624.

[228] Karvánková, P., M. G. J. Vepřek-Heijman, M. F. Zawrah, and S. Vepřek. Thermal stability of nc-TiN/a-BN/a-TiB2 nanocomposite coatings deposited by plasma chemical vapor deposition. *Thin Solid Films*, Vol. 467, No. 1–2, 2004, pp. 133–139.

[229] Mayrhofer, P. H., M. Stoiber, and C. Mitterer. Age hardening of PACVD TiBN thin films. *Scripta Materialia*, Vol. 53, No. 2, 2005, pp. 241–245.

[230] Novotny, H., F. Benesovsky, C. Brukl, and O. Schob, Titan—Bor—Kohlenstoff und Titan—Bor—Stickstoff. *Monatshefte für Chemie*, Vol. 92, 1961, pp. 403–414.

[231] Rogl, P., and J. C. Schuster. Eds. Phase Diagrams of Ternary Boron Nitride and Silicon Nitride Systems. ASM International, Materials Park, Ohio, 1992.

[232] Chaleix, L., and J. Machet. Study of the composition and of the mechanical properties of TiBN films obtained by d.c. magnetron sputtering. *Surface and Coatings Technology,* Vol. 91, No. 1–2, 1997, pp. 74–82.

[233] He, Y., I. Apachitei, J. Zhou, T. Walstock, and J. Duszczyk. Controlled plasma nitriding for an optimum balance between PACVD TiBN coating scratch resistance and substrate toughness. *Key Engineering Materials*, Vol. 373–374, 2008, pp. 312–317.

[234] Stoiber, M., C. Mitterer, T. Schoeberl, E. Badisch, G. Fontalvo, and R. Kullmer. Nanocomposite coatings within the system Ti–B–N deposited by plasma assisted chemical vapor deposition. *Journal of Vacuum Science & Technology B: Microelectronics and Nanometer Structures*, Vol. 21, No. 3, 2003, id. 1084.

[235] He, Y., J. Zhou, T. Walstock, and J. Duszczyk. Oxidation behaviour of PACVD TiBN coating at elevated temperatures. *Surface and Coatings Technology,* Vol. 204, No. 5, 2009, pp. 601–609.

[236] Wagner, J., D. Hochauer, C. Mitterer, M. Penoy, C. Michotte, W. Wallgram, *et al.* The influence of boron content on the tribological performance of Ti-N-B coatings prepared by thermal CVD. *Surface and Coatings Technology,* Vol. 201, No. 7, 2006, pp. 4247–4252.

[237] Holzschuh, H. Deposition of Ti-B-N (single and multilayer) and Zr-B-N coatings by chemical vapor deposition techniques on cutting tools. *Thin Solid Films*, Vol. 469–470, 2004, pp. 92–98.

[238] Dreiling, I., C. Raisch, J. Glaser, D. Stiens, and T. Chassé. Characterization and oxidation behavior of MTCVD Ti-B-N coatings. *Surface and Coatings Technology,* Vol. 206, No. 2–3, 2011, pp. 479–486.

[239] Yang, Q. Q., L. H. Zhao, and L. S. Wen. A study of the composition and properties of EB-ion plating Ti-B-N coatings. *Surface and Coatings Technology,* Vol. 78, No. 1–3, 1996, pp. 27–30.

[240] Tanno, Y., and A. Azushima. Frictional property of Ti-B-N coating with preferred grain orientations deposited by arc ion plating under dry condition. *Surface and Coatings Technology,* Vol. 203, No. 23, 2009, pp. 3631–3637.

[241] Neidhardt, J., Z. Czigány, B. Sartory, R. Tessadri, M. O'Sullivan, and C. Mitterer. Nanocomposite Ti-B-N coatings synthesized by reactive arc evaporation. *Acta Materialia*, Vol. 54, No. 16, 2006, pp. 4193–4200.

[242] He, J. L., S. Miyake, Y. Setsuhara, I. Shimizu, M. Suzuki, K. Numata, *et al.* Improved anti-wear performance of nanostructured titanium boron nitride coatings. *Wear*, Vol. 249, No. 5–6, 2001, pp. 498–502.

[243] Jung, D. H., H. Kim, G. R. Lee, B. Park, J. J. Lee, and J. H. Joo. Deposition of Ti–B–N films by ICP assisted sputtering. *Surface and Coatings Technology,* Vol. 174 – 175, 2003, pp. 638–642.

[244] Matthes, B., E. Broszeit, and K.H. Kloos. Wear behaviour of r.f.-sputtered TiN, TiB2 and Ti(B,N) coatings on metal forming tools in a model wear test. *Surface and Coatings Technology,* Vol. 43–44, 1990, pp. 721–731.

[245] Deng, H., J. Chen, R. B. Inturi, and J.A. Barnard. Structure, mechanical and tribological properties of d.c. magnetron sputtered TiB2 and TiB2(N) thin films. *Surface and Coatings Technology,* Vol. 76–77, 1995, pp. 609–614.

[246] Héau, C., N. Guillon, R. Y. Fillit, and J. Machet. Ultra-hard Ti-B-N coatings obtained by magnetron sputtering. *Surface and Coatings Technology,* Vol. 97, No. 1–3, 1997, pp. 60–65.

[247] Liu, Z. J., Y. H. Lu, and Y. G. Shen. Grain growth in nanocomposite Ti-B-N films during deposition: The effect of amorphous phase precipitation. *Journal of Materials Research*, Vol. 21, No. 1, 2006, pp. 82–87.

[248] Mayrhofer, P. H., H. Willmann, and C. Mitterer. Recrystallization and grain growth of nanocomposite Ti–B–N coatings. *Thin Solid Films*, Vol. 440, 2003, pp. 174–179.

[249] López-Cartes, C., D. Martínez-Martínez, J. C. Sánchez-López, A. Fernández, A. García-Luis, M. Brizuela, *et al.* Characterization of nanostructured Ti-B-(N) coatings produced by direct current magnetron sputtering. *Thin Solid Films*, Vol. 515, No. 7–8, 2007, pp. 3590–3596.

[250] Losbichler, P., C. Mitterer, P. N. Gibson, W. Gissler, F. Hofer, and P. Warbichler. Co-sputtered films within the quasi-binary system TiN-TiB2. *Surface and Coatings Technology,* Vol. 94–95, 1997, pp. 297–302.

[251] Shtansky, D. V., A. N. Sheveiko, M. I. Petrzhik, F. V. Kiryukhantsev-Korneev, E. A. Levashov, A. Leyland, *et al.* Hard tribological Ti-B-N, Ti-Cr-B-N, Ti-Si-B-N and Ti-Al-Si-B-N coatings. *Surface and Coatings Technology,* Vol. 200, No. 1–4, 2005, pp. 208–212.

[252] Heau, C., and J. P. Ter. Ultrahard Ti–B–N coatings obtained by reactive magnetron sputtering of a Ti–B target. *Surface and Coatings Technology,* Vol. 108-109, 1998, pp. 332–339.

[253] Ott, R. D., C. Ruby, F. Huang, M. L. Weaver, and J. A. Barnard. Nanotribology and surface chemistry of reactively sputtered Ti-B-N hard coatings. *Thin Solid Films*, Vol. 377, No. 378, 2000, pp. 602–606.

[254] Musil, J., and R. Daniel. Structure and mechanical properties of magnetron sputtered Zr-Ti-Cu-N films. *Surface and Coatings Technology,* Vol. 166, No. 2–3, 2003, pp. 243–253.

[255] Baker, M. A., T. P. Mollart, P. N. Gibson, and W. Gissler. Combined x-ray photoelectron/Auger electron spectroscopy/glancing angle x-ray diffraction/extended x-ray absorption fine structure investigation of TiB x N y coatings. *Journal of Vacuum Science & Technology A Vacuum Surfaces and Films*, Vol. 15, No. 2, 1997, pp. 284–291.

[256] Pierson, J. F., E. Tomasella, and P. Bauer. Reactively sputtered Ti-B-N nanocomposite films: Correlation between structure and optical properties. *Thin Solid Films*, Vol. 408, No. 1–2, 2002, pp. 26–32.

[257] Maya, L., C. E. Vallet, and J. N. Fiedor. Reactive sputtering of titanium diboride and titanium disilicide. *Journal of Vacuum Science & Technology A Vacuum Surfaces and Films*, Vol. 15, No. 4, 1997, pp. 2007–2012.

[258] Wiedemann, R., V. Weihnacht, and H. Oettel. Structure and mechanical properties of amorphous Ti-B-N coatings. *Surface and Coatings Technology,* Vol. 116–119, 1999, pp. 302–309.

[259] Matthes, B., E. Broszeit, and K. H. Kloos. Tribological behaviour and corrosion performance of Ti-B-N hard coatings under plastic manufacturing conditions. *Surface and Coatings Technology,* Vol. 57, No. 2–3, 1993, pp. 97–104.

[260] Knotek, O., R. Breidenbach, F. Jungblut, and F. Löffler. Superhard Ti-B-C-N coatings. *Surface and Coatings Technology,* Vol. 43–44, 1990, pp. 107–115.

[261] Neidhardt, J., Z. Czigány, B. Sartory, R. Tessadri, and C. Mitterer. Wear-resistant Ti-B-N nanocomposite coatings synthesized by reactive cathodic arc evaporation. *International Journal of Refractory Metals and Hard Materials*, Vol. 28, No. 1, 2010, pp. 23–31.

[262] Lu, Y. H., Y. G. Shen, Z. F. Zhou, and K. Y. Li. Effects of B content and wear parameters on dry sliding wear behaviors of nanocomposite Ti-B-N thin films. *Wear*, Vol. 262, No. 11–12, 2007, pp. 1372–1379.

[263] Mollart, T. P., J. Haupt, R. Gilmore, and W. Gissler. Tribological behaviour of homogeneous Ti-B-N, Ti-B-N-C and TiN/h-BN/TiB2 multilayer coatings. *Surface and Coatings Technology,* Vol. 86–87, 1996, pp. 231–236.

[264] Rupa, P. K. P., P. C. Chakraborti, and S. K. Mishra. Mechanical and deformation behaviour of titanium diboride thin films deposited by magnetron sputtering. *Thin Solid Films*, Vol. 517, No. 9, 2009, pp. 2912–2919.

[265] Rupa, P. K. P, P. C. Chakraborti, and S. K. Mishra. Indentation response and contact damage of hard T-B-N films deposited by magnetron sputtering. *Eurasian Journal of Analytical Chemistry*, Vol. 13, No. 1–2, 2011, pp. 81–84.

[266] Rupa, P. K. P., P. C. Chakraborty, and S. K. Mishra. Nanoindentation studies of hard nanocomposite Ti-B-N thin films. *AIP Conference Proceedings*, Vol. 1393, 2011, pp. 239–240.

[267] Rupa, P. K. P., P. C. Chakraborti, and S. K. Mishra. Structure and indentation behavior of nanocomposite Ti-B-N films. *Thin Solid Films*, Vol. 564, 2014, pp. 160–169.

[268] Mishra. S. K., A. S. Bhattacharyya, P. Mahato, and L. C. Pathak. Multicomponent Ti-Si-B-C superhard and tough composite coatings by magnetron sputtering. *Surface and Coatings Technology,* Vol. 207, 2012, pp. 19–23.

[269] Mahato, P., R. J. Singh, and S. K. Mishra. Nanocomposite Ti-Si-B-C hard coatings deposited by magnetron sputtering: Oxidation and mechanical behaviour with temperature and duration of oxidation. *Surface and Coatings Technology,* Vol. 288, 2016, pp. 230–240.

[270] Verma, D., D. Banerjee, and S. K. Mishra. Effect of silicon content on the microstructure and mechanical properties of Ti-Si-B-C nanocomposite hard coatings. *Metallurgical and Materials Transactions A: Physical Metallurgy and Materials Science*, Vol. 50,

No. 2, 2019, pp. 894–904.
[271] Kao, C. M., J. W. Lee, H. W. Chen, Y. C. Chan, J. G. Duh, and S. P. Chen. Microstructures and mechanical properties evaluation of TiAlN/CrSiN multilayered thin films with different bilayer periods. *Surface and Coatings Technology*, Vol. 205, No. 5, 2010, pp. 1438–1443.
[272] Konyashin, I. Y. PVD/CVD Technology, for coating cemented carbides. *Surface and Coatings Technology,* Vol. 71, No. 3, 1995, pp. 277–283.
[273] Oliveira, J. C., A. Manaia, J. P. Dias, A. Cavaleiro, D. Teer, and S. Taylor. The structure and hardness of magnetron sputtered Ti-Al-N thin films with low N contents (< 42 at.%). *Surface and Coatings Technology,* Vol. 200, 2006, pp. 6583–6587.
[274] Bendavid, A., P. J. Martin, E. W. Preston, J. Cairney, Z. H. Xie, and M. Hoffman, Deposition of nanocomposite thin films by a hybrid cathodic arc and chemical vapour technique. *Surface and Coatings Technology,* Vol. 201, No. 7, 2006, pp. 4139–4144.
[275] Karvankova, P., M. G. J. Veprek-Heijman, D. Azinovic, and S. Veprek. Properties of superhard nc-TiN/a-BN and nc-TiN/a-BN/a-TiB_2 nanocomposite coatings prepared by plasma induced chemical vapor deposition. *Surface and Coatings Technology,* Vol. 200, No. 9, 2006, pp. 2978–2989.
[276] Tam, P. L., Z. F. Zhou, P. W. Shum, and K. Y. Li. Structural, mechanical, and tribological studies of Cr-Ti-Al-N coating with different chemical compositions. *Thin Solid Films*, Vol. 516, No. 16, 2008, pp. 5725–5731.
[277] Yu, D., C. Wang, X. Cheng, and F. Zhang. Microstructure and properties of TiAlSiN coatings prepared by hybrid PVD Technology. *Thin Solid Films*, Vol. 517, No. 17, 2009, pp. 4950–4955.
[278] Kim, S. K., P. Van Vinh, and J. W. Lee. Deposition of superhard nanolayered TiCrAlSiN thin films by cathodic arc plasma deposition. *Surface and Coatings Technology,* Vol. 202, No. 22–23, 2008, pp. 5395–5399.
[279] Vepřek, S., S. Reiprich, and L. Shizhi. Superhard nanocrystalline composite materials: The TiN/Si3N4 system. *Applied Physics Letters*, Vol. 66, 1995, p. 2640.
[280] Li, Y. S., S. Shimada, H. Kiyono, and A. Hirose. Synthesis of Ti-Al-Si-N nanocomposite films using liquid injection PECVD from alkoxide precursors. *Acta Materialia*, Vol. 54, No. 8, 2006, pp. 2041–2048.
[281] Vaz, F., L. Rebouta, B. Almeida, P. Goudeau, J. Pacaud, J. P. Riviere, *et al.* Structural analysis of Ti1-xSixNy nanocomposite films prepared by reactive magnetron sputtering. *Surface and Coatings Technology,* Vol. 120–121, 1999, pp. 166–172.
[282] Ribeiro, E., A. Malczyk, S. Carvalho, L. Rebouta, J. V. Fernandes, E. Alves, *et al.* Effects of ion bombardment on properties of d.c. sputtered superhard (Ti, Si, Al)N nanocomposite coatings. *Surface and Coatings Technology,* Vol. 151–152, 2002, pp. 515–520.
[283] Kim, S. K., P. V. Vinh, J. H. Kim, and T. Ngoc. Deposition of superhard TiAlSiN thin films by cathodic arc plasma deposition. *Surface and Coatings Technology,* Vol. 200, No. 5–6, 2005, pp. 1391–1394.
[284] Tanaka, Y., N. Ichimiya, Y. Onishi, and Y. Yamada. Structure and properties of Al-Ti-Si-N coatings prepared by the cathodic arc ion plating method for high speed cutting applications. *Surface and Coatings Technology,* Vol. 146, No. 147, 2001, pp. 215–221.
[285] Colligon, J. S., V. Vishnyakov, R. Valizadeh, S. E. Donnelly, and S. Kumashiro. Study of nanocrystalline TiN/Si3N4 thin films deposited using a dual ion beam method. *Thin Solid Films*, Vol. 485, No. 1–2, 2005, pp. 148–154.
[286] Tang, B., Y. Wang, L. Wang, X. Wang, H. Liu, Y. Yu, *et al.* Adhesion strength of TiN films synthesized on GCr15-bearing steel using plasma immersion ion implantation and deposition. *Surface and Coatings Technology,* Vol. 186, No. 1-2, 2004, pp. 153–156.
[287] Willmann, H., P. H. Mayrhofer, P. O. A. Persson, A. E. Reiter, L. Hultman, and C. Mitterer, Thermal stability of Al-Cr-N hard coatings. *Scripta Materialia*, Vol. 54, No. 11, 2006, pp. 1847–1851.
[288] Kimura, A., M. Kawate, H. Hasegawa, and T. Suzuki. Anisotropic lattice expansion and shrinkage of hexagonal TiAlN and CrAlN films. *Surface and Coatings Technology,* Vol. 169–170, 2003, pp. 367–370.
[289] Veprek, S., S. G. Prilliman, and S. M. Clark. Elastic moduli of nc-TiN/a-Si3N4 nanocomposites: Compressible, yet superhard. *Journal of Physics and Chemistry of Solids*, Vol. 71, No. 8, 2010, pp. 1175–1178.
[290] Veprek, S., M. G. J. Veprek-Heijman, P. Karvankova, and J. Prochazka. Different approaches to superhard coatings and nanocomposites. *Thin Solid Films*, Vol. 476, No. 1, 2005, pp. 1–29.
[291] Zhang, S., H. L. Wang, S. E. Ong, D. Sun, and X. L. Bui. Hard yet tough nanocomposite coatings - Present status and future trends, *Plasma Processes and Polymers*, Vol. 4, No. 3. 2007, pp. 219–228.
[292] Ma, D., S. Ma, and K. Xu. Superhard nanocomposite Ti-Si-C-N coatings prepared by pulsed-d.c plasma enhanced CVD. *Surface and Coatings Technology,* Vol. 200, No. 1-4, 2005, pp. 382–386.
[293] Ma, S., B. Xu, G. Wu, Y. Wang, F. Ma, D. Ma, *et al.* Microstructure and mechanical properties of SiCN hard films deposited by an arc enhanced magnetic sputtering hybrid system. *Surface and Coatings Technology,* Vol. 202, No. 22–23, 2008, pp. 5379–5382.
[294] Lee, J. W., and Y. C. Chang. A study on the microstructures and mechanical properties of pulsed DC reactive magnetron sputtered Cr-Si-N nanocomposite coatings. *Surface and Coatings Technology,* Vol. 202, No. 4–7, 2007, pp. 831–836.
[295] Kim, G. S., B. S. Kim, and S. Y. Lee. High-speed wear behaviors of CrSiN coatings for the industrial applications of water hydraulics. *Surface and Coatings Technology,* Vol. 200, No. 5–6, 2005, pp. 1814–1818.
[296] Sandu, C.S., R. Sanjinés, M. Benkahoul, F. Medjani, and F. Lévy. Formation of composite ternary nitride thin films by magnetron sputtering co-deposition. *Surface and Coatings Technology,* Vol. 201, No. 7, 2006, pp. 4083–4089.
[297] Wei, R., E. Langa, C. Rincon, and J. H. Arps. Deposition of thick nitrides and carbonitrides for sand erosion protection. *Surface and Coatings Technology,* Vol. 201, No. 7, 2006, pp. 4453–4459.
[298] Wei, R., E. Langa, J. Arps, Q. Yang, and L. Zhao. Erosion resistance of thick nitride and carbonitride coatings deposited using plasma enhanced magnetron sputtering. *Plasma Processes and Polymers*, Vol. 4, 2007, pp. 693–699.
[299] Wei, R. Plasma enhanced magnetron sputter deposition of Ti-Si-C-N based nanocomposite coatings. *Surface and Coatings Technology,* Vol. 203, No. 5–7, 2008, pp. 538–544.
[300] Wei, R. In: A. Öchsner, W. Ahmed, N. Ali. Eds. Nanocomposite coatings and nanocomposite materials. Trans Tech Publications, 2008, pp. 239–2760.
[301] Lin, H. M., J. G. Duh, R. Wei, C. Rincon, and J. W. Lee. The effect of microstructure and composition on mechanical properties in thick-layered nanocomposite Ti-Si-C-N coatings. *Surface and Coatings Technology,* Vol. 205, No. 5, 2010, pp. 1460–1464.

[302] Musil, J., F. Kunc, H. Zeman, and H. Poláková. Relationships between hardness, Young's modulus and elastic recovery in hard nanocomposite coatings. *Surface and Coatings Technology,* Vol. 154, Vo. 2–3, 2002, pp. 304–313.

[303] Yau, B. S., J. L. Huang, H. H. Lu, and P. Sajgalik. Investigation of nanocrystal-(Ti1-xAlx) Ny/amorphous-Si3N4 nanolaminate films. *Surface and Coatings Technology,* Vol. 194, No. 1, 2005, pp. 119–127.

[304] Chen, W., A. Yan, C. Wang, Y. Deng, D. C. Chen, H. Xiao, *et al.* Microstructures and mechanical properties of AlCrN/TiSiN nano-multilayer coatings consisting of fcc single-phase solid solution. *Applied Surface Science*, Vol. 509, 2020, id. 145303.

[305] Pélisson, A., M. Parlinska-Wojtan, H. J. Hug, and J. Patscheider. Microstructure and mechanical properties of Al-Si-N transparent hard coatings deposited by magnetron sputtering. *Surface and Coatings Technology,* Vol. 202, No. 4–7, 2007, pp. 884–889.

[306] Shahien, M., M. Yamada, T. Yasui, and M. Fukumoto. In situ fabrication of AlN coating by reactive plasma spraying of Al/AlN powder. *Coatings*, Vol. 1, No. 2, 2011, pp. 88–107.

[307] Mazel, A., P. Marti, F. Henry, B. Armas, R. Bonnet, and M. Loubradou. Nanostructure and local chemical composition of AlN-Si3N4 layers grown by LPCVD. *Thin Solid Films*, Vol. 304, No. 1–2, 1997, pp. 256–266.

[308] Lewin, E., D. Loch, A. Montagne, A.P. Ehiasarian, and J. Patscheider. Comparison of Al-Si-N nanocomposite coatings deposited by HIPIMS and DC magnetron sputtering. *Surface and Coatings Technology,* Vol. 232, 2013, pp. 680–689.

[309] Mishra, S. K., S. Kumari, and Soni. Development of hard and optically transparent Al-Si-N nanocomposite coatings. *Surface and Interface Analysis*, Vol. 49, No. 4, 2017, pp. 345–348.

[310] Soni, S. K. Mishra, and S. K. Sharma. Influence of nitrogen partial pressure on optical properties of magnetron sputtered Al-Si-N thin films. *Thin Solid Films*, Vol. 682, 2019, pp. 1–9.

[311] Choi, H., J. Jang, T. Zhang, J. H. Kim, I. W. Park, and K. H. Kim. Effect of Si addition on the microstructure, mechanical properties and tribological properties of Zr-Si-N nanocomposite coatings deposited by a hybrid coating system. *Surface and Coatings Technology,* Vol. 259, 2014, pp. 707–713.

[312] Bobzin, K., T. Brögelmann, N. C. Kruppe, and M. Carlet. Nanocomposite (Ti,Al,Cr,Si)N HPPMS coatings for high performance cutting tools. *Surface and Coatings Technology,* Vol. 378, 2019, id. 124857.

[313] Musil, J., M. Zítek, K. Fajfrlík, and R. Čerstvý. Flexible antibacterial Zr-Cu-N thin films resistant to cracking. *Journal of Vacuum Science & Technology A Vacuum Surfaces and Films*, Vol. 34, No. 2, 2016, p. 021508.

[314] Musil, J., J. Blažek, K. Fajfrlík, and R. Čerstvý. Flexible antibacterial Al-Cu-N films. *Surface and Coatings Technology,* Vol. 264, 2015, pp. 114–120.

[315] Musil, J., S. Zenkin, S. Kos, R. Čerstvý, and S. Haviar. Flexible hydrophobic ZrN nitride films. *Vacuum*, Vol. 131, 2016, pp. 34–38.